2007

Laser Initiated Chain Reactions: The Kinetics of the Chlorine/ Cyclohexane/Oxygen Chain System

Robert Alan Forlines
Wright State University

LASER INITIATED CHAIN REACTIONS: THE KINETICS OF THE CHLORINE/CYCLOHEXANE/OXYGEN CHAIN SYSTEM

A thesis submitted in partial fulfillment
of the requirements for the degree of
Master of Science

By

ROBERT ALAN FORLINES
A.A.S., Electronics, Columbus State University, 1993
B.S., Chemistry, Columbus State University, 1996

2007
Wright State University

WRIGHT STATE UNIVERSITY

SCHOOL OF GRADUATE STUDIES

June 6, 2007

I HEREBY RECOMMEND THAT THE THESIS PREPARED UNDER MY SUPERVISION BY Robert Alan Forlines ENTITLED Laser Initiated Chain Reactions: The Kinetics of the Chlorine / Cyclohexane / Oxygen Chain System BE ACCEPTED IN PARTIAL FULFILLMENT OF THE REQUIREMENTS FOR THE DEGREE OF Master of Science.

_____

David A. Dolson, Ph.D.
Thesis Director

_____

Kenneth Turnbull, Ph.D.
Department Chair

Committee on
Final Examination

_____

David A. Dolson, Ph.D.

_____

Rubin Battino, Ph.D.

_____

Eric Fossum, Ph.D.

_____

Joseph F. Thomas, Jr., Ph.D.
Dean, School of Graduate Studies

ACKNOWLEDGEMENTS

I would like to thank my wife Cary for her infinite patience and encouragement during this adventure. Managing the responsibilities of husband, father, military research contractor (gas discharge physics, photochemistry, high voltage electronics), graduate student, homeowner, etc. is not easy and definitely takes its toll. I would like to thank my thesis advisor, David Dolson, for the many weekends he sacrificed to further this work. His devotion to this project and guidance are greatly appreciated. I would like to acknowledge the efforts of fellow students David Postell, Ben Kohn, and Ben Southerland for their assistance with data collection and GC/MS analysis. Lastly, I must acknowledge my employer for funding this effort and the input and encouragement of my coworkers and friends.

ABSTRACT

Forlines, Robert Alan. M.S., Department of Chemistry, Wright State University, 2007. Laser Initiated Chain Reactions: The Kinetics of the Chlorine/ Cyclohexane/ Oxygen Chain System.

The combination of laser photolysis with infrared chemiluminescence detection has proven an effective technique for determining the propagation rate coefficients of halogen + RH chain reactions. This thesis will extend the technique to cyclic alkanes by determining the propagation rate coefficients of the Cl_2/ cyclohexane chain system as well as the rate coefficient for the primary chain termination mechanism, $R\cdot + O_2 \rightarrow RO_2$. The following reaction scheme is supported by the kinetic analysis:

$$Cl_2 \xrightarrow{h\nu} 2Cl\cdot \qquad \text{Laser Photolysis}$$

$$Cl\cdot + RH \xrightarrow{k_1} HCl(v=1) + R\cdot \qquad \text{First Propagation Step}$$

$$R\cdot + Cl_2 \xrightarrow{k_2} RCl + Cl\cdot \qquad \text{Second Propagation Step}$$

where RH = cyclohexane, R· = cyclohexyl radical, and RCl = cyclohexyl chloride. The addition of a radical scavenger such as oxygen will terminate the chain reaction by the following elementary steps:

$$Cl\cdot + O_2 + M \xrightarrow{k_3} ClO_2 + M$$

$$R\cdot + O_2 \xrightarrow{k_4} RO_2$$

Laser photolysis/infrared chemiluminescence experiments were performed under pseudo first-order conditions on slowly flowing mixtures of cyclohexane, chlorine, oxygen, diluted in argon at reduced pressures (5 to 50 Torr). Chlorine is photolyzed by a Nd:YAG laser emitting a pulse of third harmonic (355 nm) light to initiate the chain reaction. The first propagation step is sufficiently exothermic as to generate HCl in the v = 1 vibrational energy level which subsequently returns to the ground state by fluorescence emission at 3.5 μm which is monitored via a bandpass filter with a cryogenically cooled (77 K) mercury-cadmium-telluride (HgCdTe) detector. This technique requires observation of HCl(v) *only* under the appropriate experimental conditions to determine the rate coefficients k_1, k_2, k_v, and k_4. Signal-to-noise challenges limit the technique from determining k_3, the scavenging of Cl atom by oxygen, because of the necessity of a third-body collision for this reaction.

A detailed derivation of the equations describing the time-dependent concentrations in this kinetic scheme under pseudo first-order conditions is included. Computer simulations were used to model the fluorescence intensity profile in an effort to determine the experimental parameters that best serves this study. Nonlinear least-squares fits of the fluorescence intensity profiles yield values for the rate coefficients when using the expression for [HCl(v)]. The values for the rate coefficients determined by this study were: $k_1 = (1.8 \pm 0.2) \times 10^{-10}$ cc·molecule^{-1}·sec^{-1}, $k_2 = (3.1 \pm 0.2) \times 10^{-11}$ cc·molecule^{-1}·sec^{-1}, $k_v = (1.7 \pm 0.5) \times 10^{-11}$ cc·molecule^{-1}·sec^{-1}, and $k_4 = (1.2 \pm 0.3) \times 10^{-11}$ cc·molecule^{-1}·sec^{-1}. Comparisons of these rate coefficients with literature values are presented and followed by a discussion of the successes and challenges of this technique.

This technique is useful for studying reactions of the halogen + hydrocarbon type where intermediates other than HCl(v) are difficult to monitor. Improvements in detector design could allow this technique in theory to perform real-time kinetic analysis and thus provide a better understanding of these chain systems.

TABLE OF CONTENTS

Page

LIST OF FIGURES

LIST OF TABLES

I. Introduction and Purpose

A. Chain Reactions

According to the Oxford Dictionary of Chemistry[1], a chain reaction is defined as:

" a reaction that is self-sustaining as a result of the products of one step initiating a subsequent step. Chemical chain reactions usually involve free radicals as intermediates."

This type of reaction has an initiation step where the first reactive intermediate is generated, one or more propagation steps where the reaction proceeds in a chain of interdependent steps where the product of one reaction becomes a reactant in the next, and one or more termination steps due to reaction of the intermediates with a species with a strong affinity for the intermediates.

The study of chain reactions is important in various arenas. For instance, chain reactions have been employed by the military for high power laser weapons research. To date most high power lasers require considerable amounts of electrical power to create the population inversion necessary to produce laser emission. The reaction between hydrogen and chlorine is an early example of a chain reaction employed as a chemical laser.

$$Cl_2 \rightarrow 2Cl\cdot$$
$$Cl\cdot + H_2 \rightarrow HCl + H\cdot$$
$$H\cdot + Cl_2 \rightarrow HCl(v \leq 5) + Cl\cdot$$

The chlorine is photolyzed with a flashlamp and, due to the exothermicity of the second propagation step, the hydrogen chloride produced is vibrationally excited. Laser emission can be stimulated on many of the $\Delta v = -1$ vibration-rotation transitions. Another example of a chemical laser employing chain reactions is as follows:

$$NO + F_2 \rightarrow ONF + F\cdot$$
$$F\cdot + D_2 \rightarrow DF(v) + D\cdot$$
$$D\cdot + F_2 \rightarrow DF(v) + F\cdot$$
$$DF(v) + CO_2 \rightarrow DF + CO_2(v)$$

This chain reaction[2] occurs spontaneously, simply by opening a valve to allow the reagents to mix, and produces vibrationally excited deuterium fluoride that can subsequently produce vibrationally excited carbon dioxide via energy transfer. Thus a high-power carbon dioxide laser can be made by creating a population inversion entirely by chemical reaction and alleviate the need for heavy and expensive power supplies to initiate lasing action.

One of the most common industrial chain reactions is the production of vinyl chloride by reacting chlorine radical with 1,2-dichloroethane as follows:

$$Cl\cdot + ClCH_2CH_2Cl \rightarrow HCl(v) + ClCH\cdot CH_2Cl(v)$$
$$ClCH\cdot CH_2Cl(v) \rightarrow ClCHCH_2(vinylchloride) + Cl\cdot$$

Vinyl chloride is polymerized to polyvinyl chloride (PVC) by yet another chain reaction whereby an unstable initiator decomposes to produce radicals that add to the double bond of the vinyl group. Here the initiation step that produces chlorine atoms may be a thermal dissociation or photodissociation of the 1,2 dichloroethane. The second propagation step is somewhat unusual in that it is a unimolecular dissociation of the chloroethyl radical produced in the first propagation step. The polymerization continues additively until the monomer is exhausted or competing processes terminate the chain.

Many combustion and atmospheric reactions proceed by chain mechanisms. In the troposphere, photolysis of ozone at wavelengths shorter than 319 nm contributes to the production of hydroxyl radicals by the following steps:

$$O_3 + h\nu \rightarrow O_2 + O(^1D)$$
$$O(^1D) + H_2O \rightarrow 2OH\cdot$$

Hydroxyl radicals are inert toward most constituents in the atmosphere (N_2, O_2, CO_2, H_2O, etc.), but highly reactive toward most atmospheric pollutants. Reaction with hydroxyl radicals is the primary means of their eventual destruction in the atmosphere. Hydroxyl radicals (and to a lesser extent $NO_3\cdot$) tend to react with hyrocarbons by hydrogen abstraction. Hydroxyl radicals proceed to drive tropospheric chain reactions that eventually produce NO_2.

The steady state concentration of ozone itself is maintained by the following chain reaction[3] :

$$NO_2 + h\nu \rightarrow NO + O\cdot$$
$$O\cdot + O_2 + M \rightarrow O_3 + M$$
$$O_3 + NO \rightarrow NO_2 + O_2$$

The natural presence of NO and NO_2 is due to the atmospheric reaction between nitrogen and oxygen by lightning, sunlight, etc. Combustion and industrial emissions release NO and NO_2 as well, which are believed to lead to elevated tropospheric ozone levels especially in urban/industrial areas. In the troposphere ozone is considered a pollutant and has been linked to many respiratory illnesses.

B. The Cl_2/Cyclohexane Chain System

Historically[4] thermally initiated and photo-initiated chemical chain reactions were studied experimentally by monitoring total gas pressures, determining explosion limits or by quantitative determination of end products. More recently the developments of sensitive real-time detection methods have enabled direct observations of chain carriers or other reaction intermediates.[5] These methods include mass spectrometry and a variety of optical spectroscopic methods such as atomic resonance fluorescence and tunable laser methods (absorbance, fluorescence, magnetic resonance and ionization). The use of infrared fluorescence spectroscopy of hydrogen halides to study chemical chain reactions was developed by Leone and coworkers[6-10] throughout the 1980s. In these experiments a cryogenically cooled semiconductor infrared detector observes fluorescence from one or more excited vibrational states of a hydrogen halide HX(v) product of one of the

propagation steps following pulsed laser initiation of the chain reaction. Because the time-dependent concentrations of the chain carriers are interrelated and because the rate of HX(v) production is dependent upon the X· atom concentration, the time-resolved HX(v) fluorescence also carries the propagation rate information. Accordingly one may determine chain propagation rates as well as vibrational relaxation rates from the HX(v) fluorescence observations. While this method depends upon photon emission from HX(v), radiative emission rates for the infrared transitions are rather small relative to collisional relaxation rates and usually may be omitted from the kinetic mechanism. In pseudo first-order experiments the infrared fluorescence intensity is directly proportional to the excited HX(v) concentration.

Dolson and Klingshirn[11] extended the infrared fluorescence method to measurements of termination rates in the Cl_2/HBr chain reaction terminated with the addition of NO to scavenge the predominant chain carrier, Br atoms. The present work further extends the termination rate measurements to a Cl_2/alkane (RH) chain reaction, terminated with addition of molecular oxygen. The hypothesis is that, in a well documented Cl_2/RH chain reaction system, HCl(v) fluorescence observations will enable rate measurements for $R\cdot + O_2 \rightarrow RO_2\cdot$ reactions or for $R\cdot + \cdot NO \rightarrow RNO$, as an added radical scavenger (O_2 or NO or other) scavenges the alkyl radical R· chain carrier. These reactions have some significance in atmospheric modeling efforts and in laboratory studies. Alkyl radicals are difficult to monitor directly so this method may provide an opportunity to determine rate coefficients in selected reactions without the requirement to directly observe R·. Thus, no matter the alkyl identity, the termination rates always will be determined from HCl(v) fluorescence observations.

Reactions of this type have been previously studied with cyclohexane, but no studies of the termination kinetics have been done to date. Cyclohexane is an ideal candidate to study because it extends the previous work to cyclic alkanes. Studies were done with Cl_2/butane by Nesbitt and Leone[6-8] which yielded reaction mechanisms for reactions of the halogen/hydrocarbon type that seem to fit their kinetic observations well. Using their work as a template, the following mechanism is most likely for the Cl_2/cyclohexane system terminated by addition of molecular oxygen:

$$Cl_2 + h\nu \rightarrow 2Cl\cdot \qquad \text{Initiation Step}$$

$$Cl\cdot + RH \xrightarrow{k_1} HCl(v) + R\cdot$$
$$R\cdot + Cl_2 \xrightarrow{k_2} RCl + Cl\cdot \qquad \text{Propagation and Relaxation Steps}$$
$$HCl(v) + M \xrightarrow{k_v} HCl + M$$

$$Cl\cdot + O_2 + M \xrightarrow{k_3} ClO_2\cdot + M$$
$$R\cdot + O_2 \xrightarrow{k_4} RO_2\cdot \qquad \text{Termination Steps}$$

The chlorine molecule must first be photolyzed to two chlorine atoms with a sufficiently energetic light source. Flash photolysis has been used traditionally for this task, but because of the broadband emission of flashlamps, the selectivity of this technique is rather poor. A Q-switched Neodymium:Yttrium Aluminum Garnet (Nd:YAG) laser with third harmonic (355 nm) output is sufficient to photolyze chlorine selectively. The light pulse width (~10 nsec) is quite short in comparison to the ensuing

kinetics so the reaction initiation is well defined. The ability to vary the laser pulse energy permits the variation of chlorine atom concentrations over several orders of magnitude.

Chain kinetic behavior is sometimes difficult to study due to the transient nature of the intermediates and the fact that many of the intermediates are difficult to detect. In the reaction of chlorine radical with cyclohexane, the first propagation step, the abstraction of hydrogen from cyclohexane, is sufficiently exothermic (see the calculation in the next paragraph) as to produce vibrationally excited hydrogen chloride (HCl(v)) that subsequently relaxes from the v = 1 energy level to the ground state by releasing a photon at 3.5 μm that can be detected with a cryogenically cooled (77 K) indium-antimonide (InSb) or mercury-cadmium-telluride (HgCdTe) detector. The HCl(v) time-resolved fluorescence profile in the absence of terminating species will be influenced by both k_1 and k_2 as well as the rate coefficient due to collisional (energy transfer) relaxation, k_v. It will be shown that analyses of the observed fluorescence profiles in the absence of radical scavenging (and thus chain terminating) species such as oxygen can yield experimental values of these three rate coefficients.

It is important to know if the HCl(v) produced in the Cl· + cyclohexane reaction is limited to the $v \leq 1$ vibrational states or if the reaction exothermicity also can produce higher vibrational states. V-V relaxation of higher HCl vibrational states into lower ones complicates the kinetic descriptions of the lower states. Using the standard enthalpies of formation from NIST[12] for Cl· atom (121.3 kJ/mol), HCl (-92.3 kJ/mol) and cyclohexane (-123.1 kJ/mol) and $\Delta_f H° = 52.8$ kJ/mol for the cyclohexyl radical[13], we may determine the following reaction enthalpy:

$$Cl\cdot(g) + c\text{-}C_6H_{12}(g) \rightarrow HCl(g) + c\text{-}C_6H_{11}\cdot(g) \qquad \Delta_{rxn}H^\circ = -32.3 \text{ kJ}$$

This $\Delta_{rxn}H^\circ$ magnitude is equivalent to an exothermicity of 2700 cm^{-1}, which is sufficient only to excite the v=1 level of the HCl product. There is no possibility for direct excitation of overtone HCl levels so v-v population of HCl(v=1) from higher levels cannot complicate the analysis of infrared fluorescence observations in this work.

The relaxation of HCl(v) to ground state HCl occurs mostly by collision with cyclohexane because of the energy overlap of the C-H stretch mode in cyclohexane with the v = 1 to v = 0 transition of HCl . This makes energy transfer between HCl and cyclohexane competitive with the decay of HCl(v) by emission of a photon. Collisional relaxation with argon or chlorine is inefficient even though both are available in relatively high concentrations. Under pseudo first-order conditions, other species (Cl·, R·, RCl) are too low in concentration to be of any consequence.

Braithwaite and Leone[14] demonstrated that a chlorine source such as sulfur monochloride (S_2Cl_2) could be photolyzed to yield a chlorine atom but not further participate in a chain reaction. Only the first propagation step and the vibrational relaxation step occur. When HCl(v) production is faster than HCl(v) relaxation, the HCl(v) emission profile has a rise dependent on k_1 and a decay dependent on k_v. The kinetic equations that describe the concentration of HCl(v) as a function of time are derived for various experimental conditions in the next chapter. Fits of these fluorescence profiles for a series of cyclohexane concentrations yields rise and decay coefficients that can be used to determine k_1 and k_v.

We can then borrow from the work of Nesbitt and Leone[6-8] to experimentally determine k_2. If the chain reaction is allowed to proceed by using chlorine in place of S_2Cl_2 and the experimental parameters are manipulated to allow simplification of the equation describing the time-dependent concentration of HCl(v), the ratio of k_1/k_2 can be determined from the fits. Since we will have determined k_1 previously, we will then know k_2 as well.

Klingshirn and Dolson[11] demonstrated that it is possible to determine, from the HCl(v) fluorescence profile, the rate of termination of a Cl_2/RH chain reaction through radical scavenging. For the O_2 terminated Cl_2 / RH chain reaction under steady-state conditions, the termination rate is given by $-(d[Cl\cdot]/dt + d[R\cdot]/dt) = (k_3[M][O_2][Cl\cdot] + k_4[O_2][R\cdot])$. This sum is expected to be dominated by the k_4 term at low pressures because the reactive loss of chlorine atoms proceeds via a slower termolecular reaction. An estimate of these rates may be obtained with a recommended value[15] for k_3 of 2.7×10^{-33} $cc^2 \cdot molecule^{-2} \cdot s^{-1}$, the only previously reported value[16] for k_4 is 1.3×10^{-11} $cc \cdot molecule^{-1} \cdot sec^{-1}$, and considering an oxygen partial pressure of 0.5 Torr and 20 Torr total pressure. For the stated conditions the termination rate is $-(d[Cl\cdot]/dt + d[R\cdot]/dt) = (58 \cdot s^{-1}[Cl\cdot] + 2.1 \times 10^5 \cdot s^{-1}[R\cdot])$. Except for conditions that strongly favor a high steady-state $[Cl\cdot]/[R\cdot]$ ratio, termination of the chain by reaction between cyclohexyl radical and oxygen will be the dominant route in the proposed experiments. Accordingly, chain termination rate measurements from HCl(v) fluorescence observations provide a method to determine the k_4 rate coefficient without having to detect the cyclohexyl radical directly.

II. Kinetic Equations and Analytic Solutions

In this section I will describe the derivation of useful kinetic expressions and equations that facilitate our understanding of this type of chain reaction. This analysis will yield a set of equations that describe the time dependent concentrations of the intermediate radical species. We will understand how varying the concentration of one or more reagents will affect the time dependent radical concentrations and hence the HCl(v) fluorescence emission profile. The equations can be tedious to look at and follow through, but I believe it is critical to understanding the nuances of the reactions under study. I have given much effort to explaining the progression of the mathematical analysis as I proceed in an effort to make this section more enjoyable.

A. The Chain Inhibited Scenario

It is helpful to inhibit the chain reaction in order to study the kinetics of the first step and vibrational relaxation without the added complexity of the chain and the presence of radical scavengers. In the absence of the chain, the mechanism is as follows:

$$Cl\cdot + RH \xrightarrow{k_1} HCl(v) + R\cdot$$

$$HCl(v) + M \xrightarrow{k_v} HCl + M$$

Under first-order conditions the mechanism has the form of:

$$Cl \cdot \xrightarrow{k_1'} HCl(v) \xrightarrow{k_v'} HCl \qquad (1)$$

which is the familiar textbook example of consecutive first-order reactions.

$$A \xrightarrow{k_1'} B \xrightarrow{k_v'} C \qquad (2)$$

The prime notation refers to the pseudo first-order rate coefficients where $k_1' = k_1[RH]$ and $k_v' = k_v[M]$. The rate equations for this reaction take the form of:

$$\frac{d[A]}{dt} = -k_1'[A] \qquad \frac{d[B]}{dt} = k_1'[A] - k_v'[B] \qquad \frac{d[C]}{dt} = k_v'[B]$$

We can rearrange the first rate equation and integrate to find a solution that describes the concentration of A at time t.

$$\frac{d[A]}{dt} = -k_1'[A] \;\rightarrow\; \frac{d[A]}{[A]} = -k_1' dt \;\rightarrow\; Ln\frac{[A]}{[A]_o} = -k_1' t \;\rightarrow\; \frac{[A]}{[A]_o} = e^{-k_1' t}$$

$$[A] = [A]_o e^{-k_1' t} \qquad (3)$$

However, the second differential equation, $\frac{d[B]}{dt}$, is not so easy to solve. We can make this calculus problem an algebra problem by using a matrix approach. I'll omit the prime notation and we'll just assume first order conditions. It can be shown that the time dependent concentrations of each species are given by a general solution of the form of:

$$[X]_t = x_1 e^{-\lambda_1 t} + x_2 e^{-\lambda_2 t} + x_3 e^{-\lambda_3 t} + ... \qquad (4)$$

Where the λ_i are eigenvalues (k_1, k_2, 0) of the following rate matrix:

$$\begin{bmatrix} \frac{d[A]}{dt} \\ \frac{d[B]}{dt} \\ \frac{d[C]}{dt} \end{bmatrix} = \begin{bmatrix} -k_1, 0, 0 \\ k_1, -k_2, 0 \\ 0, k_2, 0 \end{bmatrix} \begin{bmatrix} [A] \\ [B] \\ [C] \end{bmatrix}$$

More specifically, for the sequential A→B→C reaction, Eq. (4) for A and B becomes:

$$[A] = a_1 e^{-k_1 t} + a_2 e^{-k_2 t} + a_3 e^{-k_3 t} + ... \qquad (5)$$

and

$$[B] = b_1 e^{-k_1 t} + b_2 e^{-k_2 t} + b_3 e^{-k_3 t} + ... \qquad (6)$$

where a consideration of the $t = \infty$ boundary conditions, $[A]_\infty = 0 = a_3$ and $[B]_\infty = 0 = b_3$, eliminates a_3 and b_3.

$$[A] = a_1 e^{-k_1 t} + a_2 e^{-k_2 t} \qquad (7)$$

The derivative of Eq. (7) with respect to time is:

$$\frac{d[A]}{dt} = -k_1 a_1 e^{-k_1 t} - k_2 a_2 e^{-k_2 t} \qquad (8)$$

If $-k_1$ is multiplied by all terms in Eq. (7):

$$-k_1[A] = -k_1 a_1 e^{-k_1 t} - k_1 a_2 e^{-k_2 t} \qquad (9)$$

A comparison of coefficients of the $e^{-k_2 t}$ terms, $-k_1 a_2 = -k_2 a_2$, is satisfied only for $a_2 = 0$ so that $a_1 = [A]_o$ and the result of Eq. (3), $[A] = [A]_o e^{-k_1 t}$, is reproduced. We haven't learned anything new yet, but the utility of the matrix approach to solving the differential rate equations has been demonstrated.

A solution for [B] can now be determined if we recall that b_3 was eliminated and we find that the t = 0 boundary condition $[B]_o = 0 = b_1 + b_2$ leads to $b_1 = -b_2$:

$$[B] = b_1 (e^{-k_1 t} - e^{k_2 t}) \qquad (10)$$

The derivative with respect to time is:

$$\frac{d[B]}{dt} = -k_1 b_1 e^{-k_1 t} - k_2 b_2 e^{-k_2 t} \qquad (11)$$

or $$\frac{d[B]}{dt} = b_1(-k_1 e^{-k_1 t} + k_2 e^{-k_2 t}) \qquad (12)$$

But, *d[B]/dt* is also equal to:

$$\frac{d[B]}{dt} = k_1[A] - k_2[B] \qquad (13)$$

Substitute for *[A]* and *[B]* and rearrange:

$$\frac{d[B]}{dt} = (k_1[A]_o - k_2 b_1)e^{-k_1 t} + k_2 b_1 e^{-k_2 t} \qquad (14)$$

So, the coefficients of the $e^{-k_1 t}$ terms in Eqs. (14) and (12) must be equal and we can use this equality to solve for b_1.

$$k_1[A]_o - k_2 b_1 = -k_1 b_1 \qquad (15)$$

$$b_1 = \frac{k_1}{k_2 - k_1}[A]_o \qquad (16)$$

With this result,

$$\boxed{[B] = \frac{k_1}{k_v - k_1}[A]_o(e^{-k_1 t} - e^{-k_v t})} \qquad (17)$$

[B] in Eq. (17) is synonymous with $[HCl(v)]_t$, the concentration of vibrationally excited (v = 1) HCl at time t in the Cl_2/RH (inhibited chain) reaction system. This equation describes the fluorescence intensity profile observed with the chain inhibited. As the HCl(v) fluorescence intensity, I_f, is directly proportional to [B], we use the form $I_f = I_o(e^{-k_1 t} - e^{-k_v t})$, where $I_o \propto \frac{k_1}{k_v - k_1}[A]_o$, to fit the $HCl_{(v)}$ observations for the "no chain" condition. This is discussed further in the section on data collection and processing. Since $[A]_o = [A] + [B] + [C]$, and we already know [A] and [B], we can solve for [C].

$$[C] = [A]_o - [A] - [B] \qquad (18)$$

Substitute for [A] and [B] to arrive at a the equation that describes the concentration of C at time t.

$$\boxed{[C] = [A]_o(1 - e^{-k_1 t} - \frac{k_1}{k_v - k_1}(e^{-k_1 t} - e^{-k_v t}))} \qquad (19)$$

This is the concentration of vibrationally relaxed HCl; however, we do not observe this in experiments so Eq. (19) has no further use here. These equations developed in this

section are fine for sulfur monochloride (S_2Cl_2) or other reagents that can be photolyzed to produce chlorine radicals that participate in hydrogen abstraction, but cannot proceed to chain behavior. However, life gets more difficult when using chlorine and a more detailed approach is necessary.

B. The Simple Chain Scenario

Once the kinetics of the chain inhibited condition are examined, the simple Cl_2/RH chain reaction or the reaction without the presence of radical scavengers such as O_2 or NO can be studied. These radical scavengers add the complexity of termination steps to the kinetics. The mechanism for the chain reaction without the consideration of termination steps is:

$$Cl\cdot + RH \xrightarrow{k_1} HCl(v) + R\cdot$$
$$R\cdot + Cl_2 \xrightarrow{k_2} RCl + Cl\cdot$$
$$HCl(v) + M \xrightarrow{k_v} HCl + M$$

Where RH is cyclohexane, $R\cdot$ is the cyclohexyl radical, and $Cl\cdot$ is the chlorine atom. The rate equations are as follows:

$$\frac{d[Cl\cdot]}{dt} = -k_1[RH][Cl\cdot] + k_2[R\cdot][Cl_2] = -k_1'[Cl\cdot] + k_2'[R\cdot]$$

$$\frac{d[R\cdot]}{dt} = k_1[RH][Cl\cdot] - k_2[R\cdot][Cl_2] = k_1'[Cl\cdot] - k_2'[R\cdot]$$

$$\frac{d[HCl(v)]}{dt} = k_1[RH][Cl\cdot] - \sum_M k_v{}^M[M][HCl(v)] = k_1'[Cl\cdot] - k_v'[HCl(v)]$$

The primes designate pseudo first-order rate coefficients. If we use the matrix analysis approach as before, we can simplify the quest for a solution to the differential equations that yield the concentrations of the intermediate species at time t.

$$\begin{bmatrix} \frac{d[Cl\cdot]}{dt} \\ \frac{d[R\cdot]}{dt} \\ \frac{d[HCl(v)]}{dt} \end{bmatrix} = \begin{bmatrix} -k_1', k_2', 0 \\ k_1', -k_2', 0 \\ k_1', 0, -k_v' \end{bmatrix} \begin{bmatrix} [Cl\cdot] \\ [R\cdot] \\ [HCl(v)] \end{bmatrix}$$

Where the determinant of the rate matrix is:

$$\begin{vmatrix} \lambda - k_1', k_2', 0 \\ k_1', \lambda - k_2', 0 \\ k_1', 0, \lambda - k_v' \end{vmatrix} = 0$$

Solving for λ yields the following equation:

$$(\lambda - k_1' - k_2')(\lambda - k_v')\lambda = 0 \qquad (20)$$

The λ_i eigenvalues are $\lambda_1 = k_1' + k_2'$, $\lambda_2 = k_v'$, and $\lambda_3 = 0$ is the trivial solution that leads to a possible constant (steady-state) term in the $[X]_t$ concentration of Eq. (4). The eigenvalues $k_1' + k_2'$ and k_v' are the observable pseudo first-order rate coefficients that govern the time-

dependent concentrations in the Cl_2/RH chain reaction. Note that k_1' and k_2' are not separable in the proposed chain observations. The chain carrier concentrations can be described by the general Eq. (4):

$$[Cl\cdot]_t \, or [R\cdot]_t = a_1 e^{-(k_1'+k_2')t} + a_2 e^{-k_v't} + a_3 \qquad (21)$$

Because Cl· and R· are not "connected" to the relaxation of HCl(v), the a_2 coefficient is zero in Eq. (21) so that:

$$[Cl\cdot]_t = a_1 e^{-(k_1'+k_2')t} + a_3 \qquad (22)$$

Where a_3 is a constant equal to $[Cl\cdot]_{ss}$ (the steady-state concentration of chlorine atoms). Examine the limit as *t* goes to zero.

$$[Cl\cdot]_t = [Cl\cdot]_o = a_1 + a_3 = a_1 + [Cl\cdot]_{ss} \qquad (23)$$

$$a_1 = [Cl\cdot]_o - [Cl\cdot]_{ss} \qquad (24)$$

The result is:

$$[Cl\cdot]_t = ([Cl\cdot]_o - [Cl\cdot]_{ss}) e^{-(k_1'+k_2')t} + [Cl\cdot]_{ss} \qquad (25)$$

For $[R\cdot]_t = b_1 e^{-(k_1'+k_2')t} + b_3$, the limit as *t* goes to zero is $[R\cdot]_t = b_1 + b_3 = 0$ because initially the concentration of $R\cdot$ is zero. Therefore, $b_1 = -b_3$. At long time, $[R\cdot]_t = [R\cdot]_{ss} = b_3$ and it follows that $b_1 = -[R\cdot]_{ss}$. The result is:

$$[R\cdot]_t = -[R\cdot]_{ss} e^{-(k_1'+k_2')t} + [R\cdot]_{ss} \tag{26}$$

or:

$$[R\cdot]_t = [R\cdot]_{ss}(1 - e^{-(k'+k_2')t}) \tag{27}$$

We don't yet know expressions for $[Cl\cdot]_{ss}$ or $[R\cdot]_{ss}$. We do know that the steady-state approximation requires:

$$\frac{d[Cl\cdot]}{dt} = \frac{d[R\cdot]}{dt} = 0 \tag{28}$$

And from the kinetic rate equations:

$$\frac{d[Cl\cdot]}{dt} = -k_1'[Cl\cdot]_{ss} + k_2'[R\cdot]_{ss} = 0 \tag{29}$$

$$\frac{d[R\cdot]}{dt} = k_1'[Cl\cdot]_{ss} - k_2'[R\cdot]_{ss} = 0 \tag{30}$$

and thus:

$$k_1'[Cl\cdot]_{ss} = k_2'[R\cdot]_{ss} \tag{31}$$

which leads to an important relationship of proportionality:

$$\boxed{\frac{[Cl\cdot]_{ss}}{[R\cdot]_{ss}} = \frac{k_2'}{k_1'} = \frac{k_2[Cl_2]}{k_1[RH]}} \tag{32}$$

We also realize that $[Cl\cdot]_{ss} + [R\cdot]_{ss} = [Cl\cdot]_o$ and can substitute for $[Cl\cdot]_{ss}$.

$$\frac{k_2'}{k_1'}[R\cdot]_{ss} + [R\cdot]_{ss} = [Cl\cdot]_o \tag{33}$$

We now have an equation decscribing the steady-state concentration of the cyclohexyl radical.

$$[R\cdot]_{ss} = \frac{k_1'}{k_1' + k_2'}[Cl\cdot]_o \tag{34}$$

Substitute $[R\cdot]_{ss}$ into the equation for $[R\cdot]_t$ to yield an expression for the cyclohexyl radical at time t.

$$\boxed{[R\cdot]_t = \frac{k_1'}{k_1'+k_2'}[Cl\cdot]_o(1-e^{-(k_1'+k_2')t})} \qquad (35)$$

Now solve for $[Cl\cdot]_{ss}$, using Eqs. (32) and (34).

$$[Cl\cdot]_{ss} = \frac{k_2'}{k_1'+k_2'}[Cl\cdot]_o \qquad (36)$$

With some substitution in Eq. (25) we obtain the expression for the time dependent concentration of chlorine atoms.

$$\boxed{[Cl\cdot]_t = \frac{k_1'}{k_1'+k_2'}[Cl\cdot]_o e^{-(k_1'+k_2')t} + \frac{k_2'}{k_1'+k_2'}[Cl\cdot]_o} \qquad (37)$$

In an effort to obtain an equation for $[HCl(v)]$, we have two equations: a generic equation derived from the matrix approach and a kinetic equation from the rate equation.

$$\text{Generic} \rightarrow [HCl(v)] = c_1 e^{-(k_1'+k_2')t} + c_2 e^{-k_v't} + c_3 \qquad (38)$$

$$\text{Kinetic} \rightarrow \frac{d[HCl(v)]}{dt} = k_1'[Cl\cdot]_t - k_v'[HCl(v)]_t \qquad (39)$$

If the generic equation and Eq. (37) for $[Cl\cdot]_t$ are substituted into the kinetic equation, we obtain the following result:

$$\frac{d[HCl(v)]}{dt} = \frac{k_1'^2}{k_1'+k_2'}[Cl\cdot]_o e^{-(k_1'+k_2')t} + \frac{k_1'k_2'}{k_1'+k_2'}[Cl\cdot]_o - k_v'c_1 e^{-(k_1'+k_2')t} - k_v'c_2 e^{-k_v't} - k_v'c_3 \tag{40}$$

Combining the $e^{-(k_1'+k_2')t}$ terms:

$$\frac{d[HCl(v)]}{dt} = \left(\frac{k_1'}{k_1'+k_2'}[Cl\cdot]_o - k_v'c_1\right)e^{-(k_1'+k_2')t} - k_v'c_2 e^{-k_v't} - k_v'c_3 + \frac{k_1'k_2'}{k_1'+k_2'}[Cl\cdot]_o \tag{41}$$

If we take the derivative of the generic equation in Eq. (42), we have an equality between the derivative expressions in Eqs. (41) and (42) such that the first terms are equal, the second terms are equal, and so on.

$$\frac{d[HCl(v)]_t}{dt} = -(k_1'+k_2')c_1 e^{-(k_1'+k_2')t} - k_v'c_2 e^{-k_v't} \tag{42}$$

The equality of the first terms: $-(k_1'+k_2')c_1 = \frac{k_1'^2}{k_1'+k_2'}[Cl\cdot]_o - k_v'c_1$ (43)

We can now rearrange and solve for the coefficient c_1.

$$c_1 = \frac{-k_1'^2}{(k_1'+k_2')(k_1'+k_2'-k_v')}[Cl\cdot]_o \tag{44}$$

For the second terms:

$$-k_v' c_2 = -k_v' c_2 \qquad \text{no help here!} \tag{45}$$

From the equality of the third terms we can derive an expression for c_3.

$$-k_v' c_3 + \frac{k_1' k_2'}{k_1' + k_2'}[Cl\cdot]_o = 0 \tag{46}$$

$$c_3 = \frac{k_1' k_2'}{(k_1' + k_2')k_v'}[Cl\cdot]_o \tag{47}$$

We can obtain c_2 if we examine the limit of Eq. (38) as t goes to zero which yields $c_1 + c_2 + c_3 = 0$.

$$c_2 = -(c_1 + c_3) \tag{48}$$

$$c_2 = \frac{k_1'(k_v' - k_2')}{k_v'(k_1' + k_2' - k_v')}[Cl\cdot]_o \tag{49}$$

Now if we substitute for c_1, c_2, and c_3 and rearrange we obtain the equation for $[HCl(v)]_t$.

$$\boxed{[HCl(v)]_t = \frac{k_1'^2}{(k_1' + k_2')(k_1' + k_2' - k_v')}[Cl\cdot]_o\left[e^{-k_v' t} - e^{-(k_1' + k_2')t}\right] + \frac{k_1' k_2'}{(k_1' + k_2')k_v'}[Cl\cdot]_o\left[1 - e^{-k_v' t}\right]} \tag{50}$$

or from the work by Nesbitt and Leone[9]:

$$[HCl(v)]_t = HCl_{ind}[e^{-k_v't} - e^{-(k_1'+k_2')t}] + \frac{k_{chain}}{k_v'}[1 - e^{-k_v't}] \qquad (51)$$

where:

$$HCl_{ind} = \frac{k_1'^2\,[Cl\cdot]_o}{(k_1'+k_2')(k_1'+k_2'-k_v')} \qquad (52)$$

and:

$$k_{chain} = \frac{k_1'k_2'[Cl\cdot]_o}{(k_1'+k_2')} \qquad (53)$$

C. The Presence of a Radical Scavenger

Up to this point, termination processes have been omitted. Now the equations for the intermediate species concentrations will be derived taking termination by O_2 into consideration. Note that a significant feature in the simple Cl_2/RH chain reaction is the steady-state concentration term in each of $[Cl\cdot]_t$, $[R\cdot]_t$, and $[HCl(v)]_t$. Addition of a radical scavenger, such as O_2, results in the decay of these steady-state concentrations. The full mechanisms proposed are as follows:

$$Cl_2 \xrightarrow{h\nu} 2Cl\cdot$$
$$Cl\cdot + RH \xrightarrow{k_1} HCl(v) + R\cdot$$
$$R\cdot + Cl_2 \xrightarrow{k_2} RCl + Cl\cdot$$
$$Cl\cdot + O_2 + M \xrightarrow{k_3{}^M} ClO_2\cdot + M$$
$$R\cdot + O_2 \xrightarrow{k_4} RO_2\cdot$$
$$HCl(v) + M \xrightarrow{k_v{}^M} HCl + M$$

If pseudo first-order kinetics are assumed the rate equations are as follows, where primes denote pseudo first-order rate coefficients.

$$\frac{d[Cl\cdot]}{dt} = -k_1[RH][Cl\cdot] + k_2[Cl_2][R\cdot] - \sum_M k_3{}^M[O_2][M][Cl\cdot]$$

$$\frac{d[Cl\cdot]}{dt} = -(k_1' + k_3')[Cl\cdot] + k_2'[R\cdot]$$

$$\frac{d[R\cdot]}{dt} = k_1[RH][Cl\cdot] - k_2[Cl_2][R\cdot] - k_4[O_2][R\cdot]$$

$$\frac{d[R\cdot]}{dt} = k_1'[Cl\cdot] - (k_2' + k_4')[R\cdot]$$

$$\frac{d[ClO_2\cdot]}{dt} = k_3'[Cl\cdot]$$

$$\frac{d[RO_2\cdot]}{dt} = k_4'[R\cdot]$$

$$\frac{d[HCl_{(v)}]}{dt} = k_1'[Cl\cdot] - \sum_M k_v{}^M[M][HCl_{(v)}]$$

$$\frac{d[HCl_{(v)}]}{dt} = k_1'[Cl\cdot] - k_v'[HCl_{(v)}]$$

If we assume nothing more happens to $ClO_2\cdot$ and $RO_2\cdot$ during the time of experimental observations, these species can be omitted from the rate matrix without any loss of information about $[Cl\cdot]_t$, $[R\cdot]_t$, or $[HCl(v)]_t$. We may choose to include only $Cl\cdot$ and $R\cdot$ in the rate matrix and then to define $[HCl(v)]_t$ based upon the expression for $[Cl\cdot]_t$ (the integrating factor method) or we may choose to include all three of $Cl\cdot$, $R\cdot$, and $HCl(v)$ in the rate matrix and solve for $[HCl(v)]_t$ pre-exponential factors by examining the boundary conditions.

$$\begin{bmatrix} \frac{d[Cl\cdot]}{dt} \\ \frac{d[R\cdot]}{dt} \\ \frac{d[HCl(v)]}{dt} \end{bmatrix} = \begin{bmatrix} -(k_1'+k_3'), k_2', 0 \\ k_1', -(k_2'+k_4'), 0 \\ k_1', 0, -k_v' \end{bmatrix} \begin{bmatrix} [Cl\cdot] \\ [R\cdot] \\ [HCl(v)] \end{bmatrix}$$

OR

$$\begin{bmatrix} \frac{d[Cl\cdot]}{dt} \\ \frac{d[R\cdot]}{dt} \end{bmatrix} = \begin{bmatrix} -(k_1'+k_3'), k_2' \\ k_1', -(k_2'+k_4') \end{bmatrix} \begin{bmatrix} [Cl\cdot] \\ [R\cdot] \end{bmatrix}$$

Using the 3x3 matrix, the determinant takes the form:

$$\begin{vmatrix} \lambda-(k_1'+k_3'), k_2', 0 \\ k_1', \lambda-(k_2'+k_4'), 0 \\ k_1', 0, \lambda-k_v' \end{vmatrix} = 0$$

It can be shown that this determinant yields the following solution:

$$(\lambda - k_v')[(\lambda - (k_1'+k_3'))(\lambda - (k_2'+k_4')) - k_1'k_2'] = 0 \qquad (54)$$

It's clear that λ is going to have three solutions. The obvious one (λ_1) is if we assume $\lambda - k_v' = 0$. Then $\lambda_1 = k_v'$. The other two solutions will come from the quadratic solution of the terms within the square brackets. The presence of the $k_1'k_2'$ term blocks a simpler solution for λ. λ_2 and λ_3 will be referred to hereafter as λ_+ and λ_- because of the $\pm$ conditions of the quadratic equation.

$$\lambda_\pm = \frac{(k_1'+k_2'+k_3'+k_4') \pm \left[(k_1'+k_2'+k_3'+k_4')^2 - 4(k_1'k_4'+k_2'k_3'+k_3'k_4')\right]^{1/2}}{2} \qquad (55)$$

Now we have expressions for the pseudo first-order observed rate coefficients, λ_+ and λ_-, which govern the time dependent concentrations of $Cl\cdot$ and $R\cdot$. $[\mathrm{Cl}\cdot]_t$ will exhibit a double exponential decay from $[\mathrm{Cl}\cdot]_o$ with the two time constants, $\tau_+ = 1/\lambda_+$ and $\tau_- = 1/\lambda_-$, while $[\mathrm{R}\cdot]_t$ will grow with τ_+ and then decay with τ_- back to zero. We also know that if we are concerned about $HCl(v)$ that a third rate coefficient, related to vibrational relaxation, λ_1 or k_v', is present in the expression for $[HCl(v)]_t$. Let's start by using the general solution from Eq. (4), $[X]_t = x_1 e^{-\lambda_1 t} + x_2 e^{-\lambda_2 t}$, and modifying it to better describe $[Cl\cdot]_t$.

$$[Cl\cdot]_t = a_+ e^{-\lambda_+ t} + a\_e^{-\lambda\_t} \tag{56}$$

Examine the limit as *t* goes to zero.

$$[Cl\cdot]_t = [Cl\cdot]_o = a_+ + a_- \qquad \text{or} \qquad a_- = [Cl\cdot]_o - a_+ \tag{57}$$

Substitute for a_-.

$$[Cl\cdot]_t = a_+ e^{-\lambda_+ t} + ([Cl\cdot]_o - a_+)e^{-\lambda\_t} \tag{58}$$

Now we can use the general solution again to do the same for $[R\cdot]_t$.

$$\begin{aligned} [R\cdot]_t &= b_+ e^{-\lambda_+ t} + b\_e^{-\lambda\_t} \\ [R\cdot]_o &= b_+ + b_- = 0 \\ b_- &= -b_+ \end{aligned}$$

$$[R\cdot]_t = b_+ (e^{-\lambda_+ t} - e^{-\lambda\_t}) \tag{59}$$

We need to generate an expression for the coefficients a_+ and b_+. Let's try taking the derivative of $[Cl\cdot]_t$ and the kinetic expression to obtain the following relationship:

$$\frac{d[Cl\cdot]}{dt} = -a_+ \lambda_+ e^{-\lambda_+ t} - ([Cl\cdot]_o - a_+)\lambda\_e^{-\lambda\_t} = -(k_1' + k_3')[Cl\cdot]_t + k_2'[R\cdot]_t \tag{60}$$

Substitute for $[Cl\cdot]_t$ and $[R\cdot]_t$ from Eqs. (58) and (59), respectively, and combine terms to obtain the following equation:

$$\frac{d[Cl\cdot]}{dt} = -(k_1'+k_3')a_+e^{-\lambda_+ t} - (k_1'+k_3')([Cl\cdot]_o - a_+)e^{-\lambda_- t} + k_2'b_+e^{-\lambda_+ t} - k_2'b_+e^{-\lambda_- t} \tag{61}$$

Since the $e^{-\lambda_+ t}$ coefficients are equal in Eqs. (60) and (61) and the $e^{-\lambda_- t}$ coefficients are equal, we use the coefficients of the $e^{-\lambda_+ t}$ terms to solve for a_+ and b_+.

$$-a_+\lambda_+ = -(k_1'+k_3')a_+ + k_2'b_+ \tag{62}$$

$$b_+ = \frac{(k_1'+k_3'-\lambda_+)}{k_2'}a_+ \quad (63) \quad \text{or} \quad a_+ = \frac{k_2'}{(k_1'+k_3'-\lambda_+)}b_+ \quad (64)$$

These equations still contain the unknown coefficients a_+ and b_+, but we can solve for them by substituting the above equations into the equation decribing the equality of the coefficients of the $e^{-\lambda_- t}$ terms and rearranging the expression to solve for a_+ and b_+.

$$b_+ = \frac{(k_1'+k_3'-\lambda_+)}{k_2'}\left[\frac{(k_1'+k_3'-\lambda_-)}{\lambda_+ - \lambda_-}[Cl\cdot]_o\right] \tag{65}$$

and

$$a_+ = \frac{(\lambda_- - k_1' - k_3')}{(\lambda_- - \lambda_+)}[Cl\cdot]_o \qquad (66)$$

We can now substitute a_+ into the equation for $[Cl\cdot]_t$ and divide by $[Cl\cdot]_o$ to normalize the expression.

$$\boxed{\frac{[Cl\cdot]_t}{[Cl\cdot]_o} = \left[\frac{k_1' + k_3' - \lambda_-}{\lambda_+ - \lambda_-}\right]e^{-\lambda_+ t} + \left[\frac{\lambda_+ - k_1' - k_3'}{\lambda_+ - \lambda_-}\right]e^{-\lambda_- t}} \qquad (67)$$

This equation describes two decays; one due to λ_+ and the other due to λ_-. We can tell from the quadratic solution for λ_i that λ_+ will give rise to the faster decay. We can likewise substitute b_+ into the equation for $[R\cdot]_t$.

$$\boxed{\frac{[R\cdot]_t}{[Cl\cdot]_o} = \frac{(\lambda_+ - k_1' - k_3')(k_1' + k_3' - \lambda_-)}{k_2'(\lambda_+ - \lambda_-)}\left[e^{-\lambda_- t} - e^{-\lambda_+ t}\right]} \qquad (68)$$

Now all that remains is to solve for $[HCl(v)]_t$. We can once again customize the general solution to better describe $[HCl(v)]_t$.

$$[HCl(v)]_t = c_+ e^{-\lambda_+ t} + c_- e^{-\lambda_- t} + c_v e^{-k_v' t} \qquad (69)$$

If we examine the limit as *t* goes to zero:

$$[HCl(v)]_o = c_+ + c_- + c_v = 0$$
$$c_v = -(c_+ + c_-) \tag{70}$$

All we need are expressions for c_+ and c_- to generate an equation describing the time dependent concentration of $[HCl(v)]$. Substitute $-(c_+ + c_-)$ for c_v in Eq. (69) for $[HCl(v)]_t$ and differentiate the expression.

$$\frac{d[HCl(v)]}{dt} = -c_+\lambda_+ e^{-\lambda_+ t} - c_-\lambda_- e^{-\lambda_- t} + (c_+ + c_-)k_v' e^{-k_v' t} \tag{71}$$

And the kinetic expression from the proposed mechanism is:

$$\frac{d[HCl(v)]}{dt} = k_1'[Cl\cdot] - k_v'[HCl(v)] \tag{72}$$

Substitute for $[Cl\cdot]$ and $[HCl(v)]$ and use the equality of the $e^{-\lambda_+ t}$ terms in Eqs. (71) and (72) to solve for c_+.

$$-c_+\lambda_+ = k_1'\left[\frac{k_1' + k_3' - \lambda_-}{\lambda_+ - \lambda_-}\right][Cl\cdot]_o - k_v' c_+ \tag{73}$$

$$c_+ = \frac{k_1'(k_1'+k_3'-\lambda_-)}{(\lambda_+ - \lambda_-)(k_v'-\lambda_+)}[Cl\cdot]_o \tag{74}$$

And from the equality of the $e^{-\lambda_- t}$ terms we can combine terms, rearrange the expression, and solve for c_-.

$$c_- = \frac{k_1'(\lambda_+ - k_1'-k_3')}{(\lambda_+ - \lambda_-)(k_v'-\lambda_-)}[Cl\cdot]_o \tag{75}$$

It is apparent that we will also need an expression for $c_+ + c_-$ as well.

$$c_+ + c_- = \frac{k_1'(k_1'+k_3'-\lambda_-)(k_v'-\lambda_-) + k_1'(\lambda_+ - k_1'-k_3')(k_v'-\lambda_+)}{(\lambda_+ - \lambda_-)(k_v'-\lambda_+)(k_v'-\lambda_-)}[Cl\cdot]_o \tag{76}$$

We have everything we need to develop the expression for $[HCl(v)]_t$ in Eq. (77).

$$\boxed{\frac{[HCl(v)]_t}{[Cl\cdot]_o} = Ae^{-\lambda_+ t} + Be^{-\lambda_- t} - (A+B)e^{-k_v' t}} \tag{77}$$

$$\boxed{A = \frac{k_1'(k_1'+k_3'-\lambda_-)}{(\lambda_+ - \lambda_-)(k_v'-\lambda_+)}} \tag{78}$$

$$\boxed{B = \frac{k_1'(\lambda_+ - k_1' - k_3')}{(\lambda_+ - \lambda_-)(k_v' - \lambda_-)}} \qquad (79)$$

We now have a thorough development of the kinetic equations for the proposed terminated chain mechanism. The equation for $[HCl(v)]_t$ may be used with a set of known and estimated rate coefficients to simulate the experimental observations and to find the optimal conditions under which to measure the rate coefficients. This same equation will be used to develop fits of the $[HCl(v)]$ fluorescence intensity profiles and to determine the kinetic rate coefficients. It can be shown that in the limit where $k_1'+k_2' >> k_3'+k_4'$, the observed rate coefficients, λ_+ and λ_-, have limiting values of $\lambda_+ \approx k_1'+k_2'$ and $\lambda_- \approx k_3'+k_4' \approx k_4'$. This simplification is useful for determining k_4 from the HCl(v) fluorescence observations.

D. Chain Simulations

As is so often the case, experiment preparation is much more labor intensive than the relatively straight-forward data collection. Selection of the optimal experimental parameters is usually a trade off between reasonable signal-to-noise ratio, ideal reagent concentrations, etc. and the limitations of the apparatus available. Computer simulations are valuable tools for selecting experimental conditions in a time efficient manner and without wasting reagents.

1. Simulations in Excel

The consideration of reagent concentrations and other experimental conditions began with a simple Excel spreadsheet and graph. The spreadsheet presented in figure 1

allows entry of reactions that participate in propagation, termination, and vibrational relaxation and a column of the rate coefficients for these processes. The rate coefficients for these steps were compiled from published data or estimated from similar starting reagents and are in units of microsecond^{-1}·Torr^{-1}. There is also a column of concentrations for cyclohexane (RH), chlorine (Cl_2), oxygen (O_2), and argon (Ar) in units of Torr. A pseudo first-order excess of reagents over radical species is assumed, and Eq. (77) is plotted for the entered partial pressure values.

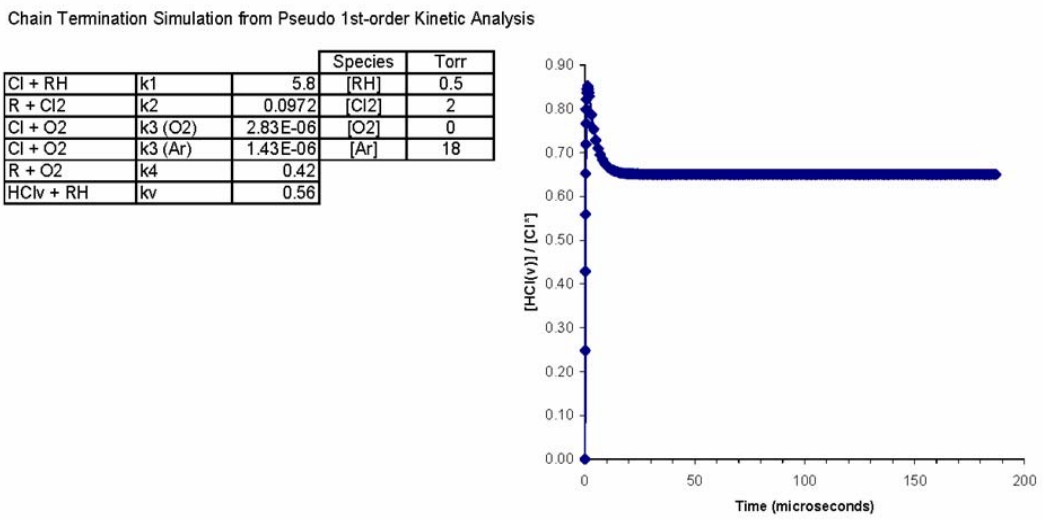

Figure 1: A typical Excel spreadsheet simulation.

This simulation provides a fast way of determining rough concentrations to push the reaction into yielding an HCl(v) profile that meets the needs of the study. The limitation with this simulator is that it is unable to account for reagent depletion and assumes that the concentrations of cyclohexane, chlorine, argon, and oxygen stay

constant. Second-order kinetic processes also are ignored here, such as Cl· reacting with the RCl product. Rates for second-order processes scale with the square of the laser pulse energy.

2. The GEAR Iterator

The GEAR iterator[17] is a FORTRAN based algorithm that has been available for many years. There are probably better simulators available as GEAR is a bit cumbersome and dated, but it works reasonably well. The chemical equations, initial concentrations, and rate coefficients are entered into a file using PRGEAR. GEAR does not specify units so consistency must be maintained by the user. Concentrations were entered in units of Torr and the time was in "units" which can be assumed to be microseconds when we use rate coefficients in units of microsecond^{-1}·Torr^{-1}. PRGEAR stores the mechanism information in a .GEA file. When GEAR is started it will prompt the user for this file and give an opportunity to change the rate coefficients, initial concentrations, and time length. The GEAR iterator essentially converts the chemical equations which are in a differential form to an integrated data set. The user can select which species to plot as concentration (in Torr) vs. time (in microseconds) and then save the simulation data with a file name including the .txt or .dat extensions for exporting data. The GEAR iterator keeps track of reagent concentrations and determines reagent depletion rates so that the simulations reflect reagent exhaustion if it is evident. The number of data points collected per given time interval depends upon the rate of change of the profiles with rapid changes requiring more data points and gradual changes proportionately less.

One drawback to GEAR is that the plotted species are often mislabeled. The first column in the data saved for export is time and the subsequent columns are the species concentrations in the order selected. There are no labels or file headers so taking notes is recommended. Once the concentrations of the reagents are narrowed down in the Excel simulator, a trial in GEAR will be useful to check for the severity of reagent depletion. Table 1 contains experimental values of k_1 and k_v from this work. GEAR predictions are presented along with experimental observations in chapter IV.

Table 1 Data used for GEAR simulations

Reaction	Rate Coefficient*
$Cl\cdot + RH \rightarrow HCl(v) + R\cdot$	5.8 (my k_1)
$R\cdot + Cl_2 \rightarrow RCl + Cl\cdot$	0.2203 (k_2 from Nesbitt & Leone[8])
$HCl(v) + RH \rightarrow HCl + RH$	0.5605 (my k_v)
$HCl(v) + Cl_2 \rightarrow HCl + Cl_2$	1.81×10^{-4} (Leone[18])
$HCl(v) + Ar \rightarrow HCl + Ar$	1.1×10^{-7} (Leone[18])
$HCl(v) + O_2 \rightarrow HCl + O_2$	1.07×10^{-4} (Leone[18])
$HCl(v) + Cl\cdot \rightarrow HCl + Cl\cdot$	0.2689 (Leone[18])
$HCl(v) + RCl \rightarrow HCl + RCl$	0.5605 (should be similar to my k_v)
$HCl(v) + R\cdot \rightarrow HCl + R\cdot$	0.5605 (should be similar to my k_v)
$HCl(v) + HCl \rightarrow HCl + HCl$	8.42×10^{-4} (Leone[18])
$R\cdot + O_2 \rightarrow RO_2$	0.4212 (k_4 from Platz et al[16])
$Cl\cdot + O_2 + Ar \rightarrow ClO_2 + Ar$	1.43×10^{-6} (Atkinson et al[19])
$Cl\cdot + O_2 + O_2 \rightarrow ClO_2 + O_2$	2.83×10^{-6} (Sander et al[15])
$Cl\cdot + O_2 + Cl_2 \rightarrow ClO_2 + Cl_2$	1.43×10^{-6} (Atkinson et al[19])

* The rate coefficients are in units of $\mu sec^{-1} \cdot Torr^{-1}$ except for the last three termolecular reactions which are in units of $\mu sec^{-1} \cdot Torr^{-2}$.

III. Experimental

A. Reagent Flow Calibrations

The partial pressure of each reagent must be known accurately and controlled in a reproducible manner in the experimental work. This is achieved by using mass flow controllers (MFCs) in conjunction with a flow control power supply/readout (MKS Instruments model 247D) and manual control (via a needle valve) of the photolysis cell pressure. The sensors in the MFCs read out a voltage (generally something like 0 to 10 Volts full range) that corresponds to the range from 0 to the full-scale rating of the mass flow controller. The controllers are routinely calibrated for nitrogen by the manufacturer unless otherwise specified; however, they are calibrated for the actual gases used for each experiment as described in the next few paragraphs.

It is customary for the readout to display in standard volume units per time such as standard cubic centimeters per minute (sccm). This unit is rather curious because it doesn't have the appearance of a true mass flow rate unit (like g/min), but has been used for years for conceptual reasons. However by using the label *standard* we are specifying a volume flow rate (which is pressure and temperature dependent) at a standard condition defined as 273.15 Kelvins and a pressure of 1 atmosphere. Since we are working at room temperature and under rarefied conditions in the cell, we can assume ideal gas behavior and use the ideal gas equation to solve for the rate of moles of gas flowing per minute.

Simply multiplying this result by the molar mass (g/mol) of the reagent gas yields units of grams per minute (g/min). So sccm is in essence a unit proportional to mass flow.

Because the MFC is calibrated for nitrogen, a gas correction factor is needed to properly interpret the display when using a different gas. We can eliminate the need for a gas correction factor and periodic factory calibration by measuring the rate of the photolysis cell pressure rise (with the photolysis cell's pressure transducer and a stopwatch) at a series of MFC settings and generating a calibration plot of dP/dt versus MFC setting for each reagent gas. These plots are generally linear and a linear least squares fit of these plots yields a slope and intercept that can be used to convert the MFC readout to dP/dt and vice versa by the following equation:

$$\frac{dP}{dt} = (slope\ x\ MFC\ readout) + y\text{-}intercept \qquad (80)$$

By using this method, we can calibrate and verify the condition of the MFCs for any reagent gas and the units of the readout become irrelevant. If we know the target cell pressure of the experiment and the sum of the dP/dt values for all gases flowing, we can calculate the partial pressures of the individual reagent gases.

$$Reagent\ Gas\ Partial\ Pressure[P] = \frac{dP/dt}{\sum dP/dt} \times\ Cell\ Pressure \qquad (81)$$

In addition to the calibrations, a zero flow photolysis cell leak rate was also measured. The MFCs were calibrated before each experimental run and the results were

incorporated into a spreadsheet used to summarize the experimental parameters which will be described in the next section.

B. The Test Spreadsheet

A spreadsheet created in Excel was updated before each experimental session as a guide. Figure 2 is a typical example. The yellow fields are where data entry is required. Most of the fields have enough descriptive annotation to make their role obvious. There are two entries for the date if the calibration and experiment happen to be on different days. The zero flow leak rate is included to correct for any inherent dP/dt from cell leak. The slopes and intercepts come from the calibrations which are entered from a separate worksheet, but within the same file. A column for a quadratic coefficient has been included because some condensable gases cause the MFC to exhibit a nonlinear response. The line labeled "BR* decay…" and the two preceding lines are remnants from an earlier version and are ignored. This is a generic spreadsheet that we use for various kinetic studies and requires that flexibility, but the quadratic coefficient columns will contain zeroes for this study. We aren't that concerned about the target MFC readings because we simply vary them to achieve the partial pressures of interest that are calculated and tabulated further down the sheet.

Flow/Pressure Targets for experiments on: 11/17/2006 Forlines/Dolson

These entries come from the zero-flow leak-up rate, thermometer reading, and the slope and intercept from plots of dP/dt vs. flow reading from the calibrations.

Calibration date: 11/17/2006

zero flow dP/dt = 4.44E-05 **Torr/sec** **T=** 25.1 **Celsius**

	intercept	slope	quad. coef.	% gas in mix	FC#
Argon	3.2567E-02	2.5148E-02	0	100.00%	1
***c*-C_6H_{12}**	7.9640E-05	6.8717E-03	0	100.00%	3
Cl_2	2.7291E-02	2.3463E-02	0	100.00%	4

Vary the target readings to achieve the individual species dP/dt below.

	target rdgs	target rdgs	target rdgs	target rdgs	target rdgs	target rdgs	target rdgs
Argon	200	200	200	200	200	200	200
***c*-C_6H_{12}**	1.00	2.00	3.00	4.00	5.00	6.00	7.00
Cl_2	22.0	22.0	22.0	22.0	22.0	22.0	22.0

Conversion of target readings to dP/dt

dP/dt = target reading x slope + intercept

	dP/dt	dP/dt	dP/dt	dP/dt	dP/dt	dP/dt	dP/dt
Argon	5.0622	5.0622	5.0622	5.0622	5.0622	5.0622	5.0622
***c*-C_6H_{12}**	0.0070	0.0138	0.0207	0.0276	0.0344	0.0413	0.0482
Cl_2	0.5435	0.5435	0.5435	0.5435	0.5435	0.5435	0.5435
total dP/dt	5.6127	5.6195	5.6264	5.6333	5.6402	5.6470	5.6539

Enter the target pressure (in Torr). Other concentrations will automatically be calculated.

Pressure Target	20.000	20.024	20.049	20.073	20.098	20.122	20.147

Pressure of species = [dP/dt of species x Pressure target] / total dP/dt

Pressure of Species (Torr)							
Argon	18.039	18.039	18.039	18.039	18.039	18.039	18.039
***c*-C_6H_{12}**	0.0248	0.0493	0.0737	0.0982	0.1227	0.1472	0.1717
Cl_2	1.9366	1.9366	1.9366	1.9366	1.9366	1.9366	1.9366
Total Pressure	20.000	20.024	20.049	20.073	20.098	20.122	20.147

Linear flow rate = [dP/dt total x tube volume] / [tube cross-sectional area x total pressure]
Minimum flow rate for gas replenishment in 1cm beam diameter and 10 Hz rate is 10 cm/sec.

Flow Rate (cm/sec)	10.0	10.0	10.0	10.0	10.0	10.0	10.0
Laser Energy (mJ)	2	2	2	2	2	2	2
		2/2	2	??/2	2	1.5/2	2
$[Cl]_0$ atoms/cc	9.7441E+13	9.7441E+13	9.7441E+13	9.7441E+13	9.7441E+13	9.7441E+13	9.7441E+13
$[Cl]_0$ Torr	0.0030	0.0030	0.0030	0.0030	0.0030	0.0030	0.0030
Pseudo 1st-Order Ratio							
$[c\text{-}C_6H_{12}]/[Cl]_0$	8.2	16.4	24.5	32.7	40.8	48.9	57.1
$[Cl_2]/[Cl]_0$	643.9	643.9	643.9	643.9	643.9	643.9	643.9

Cl quantum yield	2	These values are used in the determination of $[Cl]_0$ in line 31
sigma (σ/cm^2)	1.60E-19	BE AWARE that any changes made here will affect the $[Cl]_0$
path (cm)	20	values calculated from Planck's law and Beers law.

Figure 2: A typical test spreadsheet.

The bulk of the pressure target is due to argon which is employed as a carrier gas for reagents with vapor pressure insufficient to provide adequate MFC backing pressure and to remove excess translational energy (heat) from the photochemically produced chlorine atoms. The rate equation for the collision of a chlorine atom with argon is:

$$Rate = k_{hs}[Ar][Cl\cdot] \tag{82}$$

Where k_{hs} is the hard-sphere rate coefficient ($\sim 3x10^{-10}\, cc \cdot molecule^{-1} \cdot s^{-1}$ or $1x10^{7}\, s^{-1} \cdot Torr^{-1}$). Since the argon partial pressure will be dominant we can assume pseudo first-order kinetics.

$$k_{firstorder} = k_{hs}[Ar] \tag{83}$$

$$Rate = k_{firstorder}[Cl\cdot] \tag{84}$$

If argon has a partial pressure of 40 Torr, we may calculate $k_{firstorder} = 4x10^{8}\, s^{-1}$, and the collision interval is $\tau =$ $k_{first\text{-}order}^{-1}$ = 2.5 nsec between collisions. Since the detector response is ~200 nsec, we have ~80 collisions in the detector rise time or ~80 opportunities for chlorine atoms to transfer excess translational energy to argon during the detector response time. If we think about this in terms of interactions with argon versus interactions with cyclohexane, we have roughly 400 collisions with argon for

every collision with cyclohexane at 100 milliTorr. This is well more than adequate to assume thermalization of the chlorine radical species.

The entry for the laser energy is used to calculate the chlorine atom concentration, [Cl·], using the Beer-Lambert law and Einstein's expression for photon energy. On later versions of the spreadsheet a field for the laser wavelength is included for use in the calculation of $[Cl\cdot]_o$. Additionally the laser light path length, absorption cross-section, and photolysis quantum yield must be entered for the $[Cl\cdot]_o$ calculation. The laser beam path across the cell is 20 cm. The photolysis quantum yield , Φ, for Cl_2 is two chlorine atoms for each 355nm photon absorbed (Φ = 0.8 for S_2Cl_2 at 266 nm)[20]. The absorption cross-section of chlorine from the literature[21] is 1.60×10^{-19} cm^2 at 355 nm (1.64×10^{-17} cm^2 for S_2Cl_2 at 266 nm). This literature reference provides a table of extinction coefficients for each of a series of wavelengths in units of $M^{-1}\cdot cm^{-1}$ which can be readily converted to the absorption cross-section in units of cm^2 by multiplying by 3.82×10^{-21} from Okabe's table[22] A-3. The linear flow velocities for the experimental conditions are calculated from the spreadsheet entries and cell dimensions. Linear flow velocities of at least 10 cm/sec are desirable so that a fresh gas mixture is present for each laser shot from the 10 Hz Nd:YAG laser. The calculation of $[Cl\cdot]_o$ is described more fully in the next chapter, and is necessary for the evaluation of pseudo first-order conditions. The entries for $[c\text{-}C_6H_{12}]/[Cl\cdot]_o$ and $[Cl_2]/[Cl\cdot]_o$ near the bottom of the table in Figure 2 are desired to be as large as is possible within other constraints. Ratios in excess of 10 are required so that a rate coefficient might be determined with less than 10 % error. Chain reactions further degrade the calculated pseudo first-order excess. This spreadsheet is

extremely useful when planning an experiment and serves as a guide when collecting data.

C. Reagent Preparation and Storage

The argon used for this study is ultra high purity grade (99.999%) from a gas cylinder plumbed directly to a MFC. The chlorine was purchased in high purity (99.99%) in a lecture bottle and purified by vacuum distillation before being transferred to a 12 liter glass bulb. Cylohexane (c-C_6H_{12}) was purchased in HPLC grade (≥ 99.9 %) from Sigma-Aldrich. Cyclohexane was added (approximately 100mL) to a round bottom flask with a straight neck and connected to the vacuum system via a Cajon UltraTorr union. The sample was degassed three times by the freeze-pump-thaw technique. Cyclohexane has a high enough vapor pressure (87 Torr) to provide sufficient gas flow through the MFC for this study. Sulfur monochloride was obtained in high purity from Sigma-Aldrich.

D. The Photolysis Cell

Figure 3 shows a diagram of the photolysis reaction cell. The chain reactions of interest are carried out in a pyrex glass cell of approximately 40mm in outside diameter and an internal volume of 450 cm^3. There is a single Pyrex inlet for the reagents at the top of the cell and an outlet for pumping and pressure control at the bottom of the cell. The pumping port at the bottom of the cell is via a manifold with a coarse gas valve and a needle valve for fine control of the cell pressure. This works in lieu of a more expensive exhaust throttle valve and controller. The laser beam enters the cell by way of a 38 mm

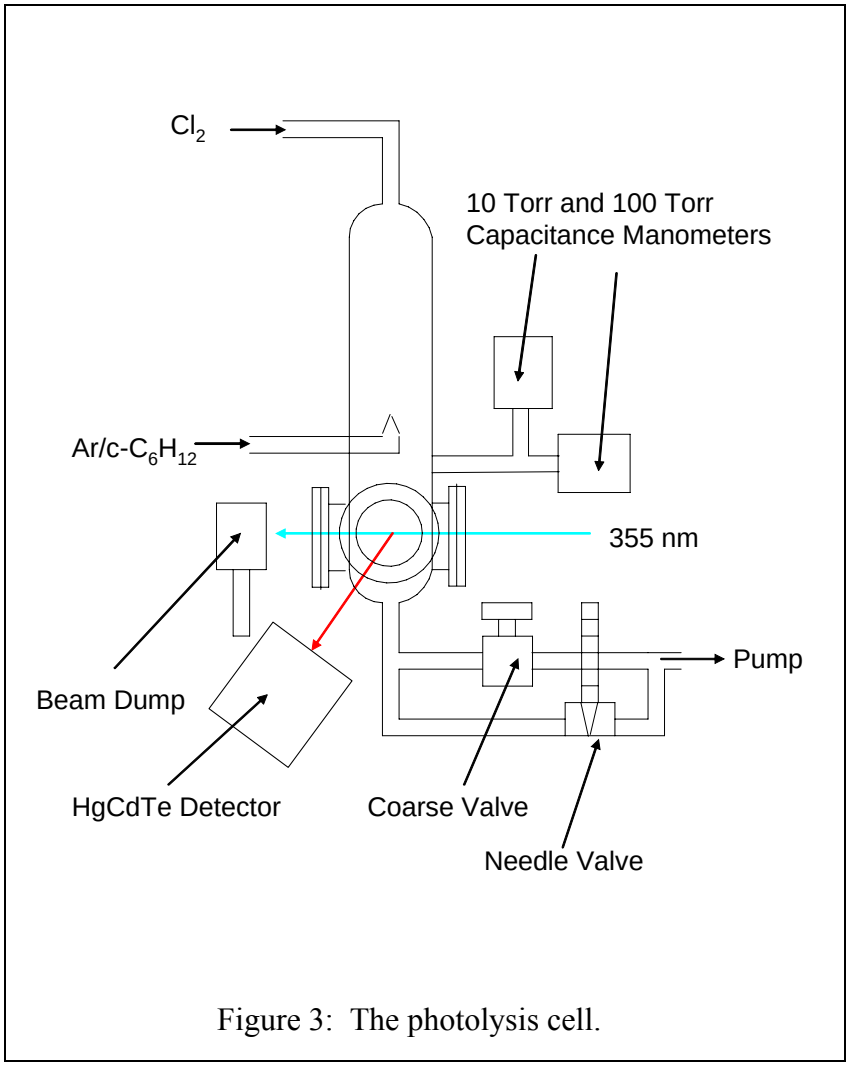

Figure 3: The photolysis cell.

fused silica window that is sealed to each side of the cell with a glass o-ring joint and a Viton o-ring. A 38 mm salt (KCl) window is sealed to the cell with Apiezon-W black wax perpendicular to the fused silica window for detection of the vibrationally excited HCl emission.

Two capacitance manometers (10 Torr and 100 Torr pressure range) are sealed via Cajon UltraTorr fittings to a side port to monitor the pressure of the cell. The 0-10 Vdc range of these capacitance manometers is measured with a digital multimeter

(DMM). Either transducer (range) may be selected by flipping a switch on a selector box wired between the DMM and the transducers.

The cell was pumped by a 500 L/min. rotary vane vacuum pump with a liquid nitrogen cooled foreline trap (77^{o}K) installed at the inlet to prevent backstream contamination of the cell with pump oil and to protect the pump from corrosive gases. The trap was isolated by valves at the end of each day and allowed to gradually warm to room temperature while purging with dry nitrogen. The dry nitrogen stream removes condensed gases from the trap as they boil. The purge is then bubbled through a flask of sodium hydroxide solution via copper tubing to neutralize the trapped gas before allowing it to exhaust by way of the fume hood.

When not in use, the cell is pumped with an oil diffusion pump with a rotary vane backing pump. These pumps are also protected with a liquid nitrogen cooled foreline trap.

E. Laser and Optics

The chain reaction is initiated using a laser pulse sufficiently energetic to dissociate the chlorine molecule into two chlorine atoms. The Cl_2 dissociation energy required as per Okabe's book[14], is 2.479 eV or 3.966 x 10^{-19} J. Using the equation for the energy of a photon ($E = hc/\lambda$) we calculate that a photon with 500 nm wavelength or shorter is required to dissociate Cl_2. We achieved this by employing the third harmonic (355 nm) of a pulsed Nd:YAG laser. Our laser is of the older unstable resonator design which produces a doughnut-shaped beam profile where the center is darker than the outer

edges of the 6mm diameter beam. This beam profile is not problematic as long as the experiment is conducted under pseudo first order conditions.

The third harmonic is produced colinearly with the fundamental wavelength (1064 nm) and the second harmonic (532 nm) which are separated by a Pellin-Broca prism and terminated into a beam dump.

The concentration of chlorine atoms is conveniently controlled by varying the flash lamp energy control while measuring the laser output energy. The relationship between laser pulse energy and chlorine atom concentration is described in the following equations. Photolysis of Cl_2 at 355 nm is used as an example. The energy of one photon is $E = hc/\lambda$, so the number of photons in the laser pulse is simply :

$$\boxed{\#\ photons = \frac{E_{pulse}\lambda}{hc}} \qquad (85)$$

The concentration of chlorine atoms is given by Eq. (86).

$$\boxed{[Cl\cdot]_o = \frac{\#\ photons * \ fraction * QY}{volume}(atoms/cc)} \qquad (86)$$

Where "fraction" is the fraction of photons absorbed, which comes from the Beer-Lambert law.

$$\text{Transmittance} = I/I_o = e^{-\sigma N l} \qquad (87)$$

The fraction of photons absorbed is $1 - I/I_o$ or $1 - e^{-\sigma N l}$, where σ is the absorption cross-section (σ_{355nm} = 1.60 x 10^{-19} cm^2), N is the molecular number density (3.24 x 10^{16} molecules/cc = 1 Torr), and *l* is the path length through the tube (20 cm). So to solve for the fraction of photons absorbed in our cell the equation is :

$$\boxed{fraction = 1 - e^{-0.1037 * Cl_2 \ pressure}} \qquad (88)$$

The quantum yield (QY) is 2 Cl atoms per photon absorbed. The estimated beam area is 1 cm^2 so the volume is 1 cm^2 times the 20 cm path length or 20 cm^3. The following equation is useful for obtaining the concentration of chlorine atoms in Torr.

$$P_o\,(Cl\cdot)/\,Torr = [Cl\cdot]_o/(3.24 \text{ x } 10^{16} \text{ atoms/cc}) \qquad (89)$$

When sulfur monochloride is used instead of chlorine for the chlorine radical source, the fourth harmonic (266nm) of the laser will be necessary to remove a chlorine atom, the quantum yield will be 0.8 instead of 2, and the absorption cross-section will have to be changed from 1.6 x 10^{-19} cm^2 to 1.64 x 10^{-17} cm^2.

F. Detector and Filters

The vibrationally excited HCl fluorescence at 3.5 μm is detected with a detector such as indium antimonide (InSb) or mercury-cadmium-telluride (HgCdTe) cooled to

77 K with liquid nitrogen to lower the background noise threshold. A photoconductive HgCdTe detector was used for this work, but future studies may benefit from the higher sensitivity of the photovoltaic InSb detector. The resistance of the 4 mm x 4 mm HgCdTe detector exhibits a negative temperature dependence, or rather, its resistance decreases when exposed to infrared radiation. The rise time of this detector is 200 nanoseconds. The window on the detector is ZnSe and a light gathering lens is placed between the window and the detector element. This detector has a spectral range of from 2 to 19 μm. Because of the relatively weak fluorescence we sought to avoid optical losses and expense of focusing optics and position the detector as close to the salt window on the photolysis cell as possible.

The voltage drop across the detector element was amplified before the data was collected in order to improve the signal to noise ratio. To discriminate against sources of radiation other than the HCl(v=1) fluorescence, IR band pass filters were employed. One had a wider bandpass (~1300 cm^{-1} FWHM) and another a narrower bandpass (~200 cm^{-1} FWHM). The wider band pass would allow more light for better signal to noise, but was found to allow C-H stretch emission from cyclohexane or cyclohexyl chloride that also occurs in this spectral region (see Figure 4). We determined this by running experiments with each filter independently and taking data both with and without a cold gas filter (CGF), consisting of a cell of 1 cm in length and filled with HCl at a pressure of 200 Torr. This filter efficiently blocks HCl(v=1) emission so that interference from other emission sources may be assessed (see Figure 5). The narrow band interference filter provides better isolation of the HCl(v=1) emission and so was used for all data collection.

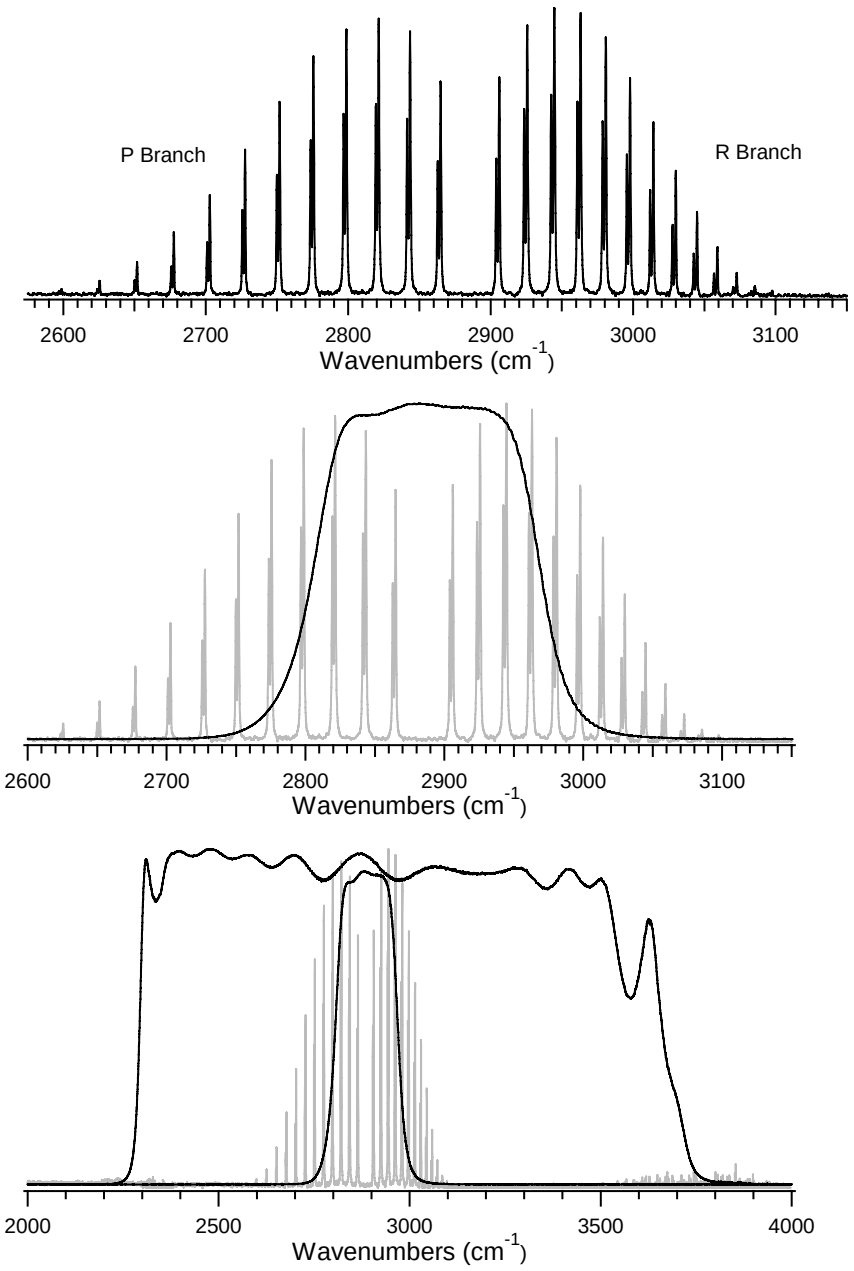

Figure 4: Filter transmission plots. The middle profile is the narrow band filter. The lower profile is the wide and narrow band filter superimposed for comparison.

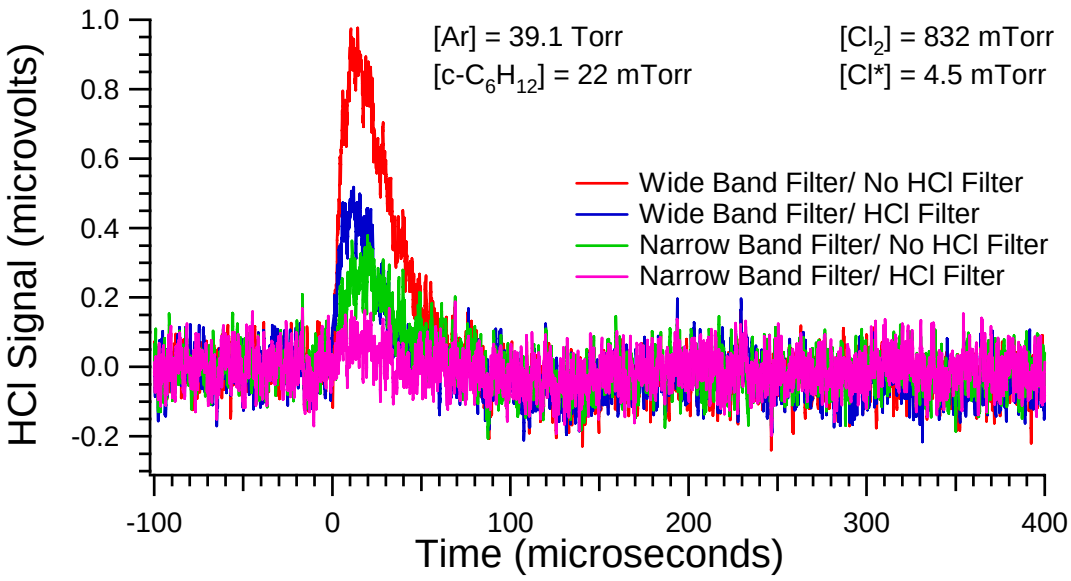

Figure 5: Filter blocking characteristics with and without a HCl cold gas filter.

G. Data Collection and Processing

Amplified HgCdTe detector waveforms were collected on an oscilloscope (LeCroy 6030) and averaged for 5000 to 20,000 laser pulses, determined by signal-to-noise and experimental constraints. The oscilloscope has an analog bandwidth of 300 MHz and a digital sampling rate of 1GS/s. The oscilloscope was externally triggered with a photodiode aimed to collect scattered light from the outlet of the Nd:YAG laser. A background trace was collected (with the laser blocked) to be subtracted from the data files in an effort to eliminate electrical dark noise. This oscilloscope has the ability to save files in binary or ASCII format on portable USB (universal serial bus) removable media. Most of our files were saved in binary format to conserve memory and were later converted to ASCII with a free program that the oscilloscope manufacturer offers (ScopeExplorer).

All of the data were manipulated and prepared for publication using IGOR (Wavemetrics version 5.11) data reduction software. Once the background file was subtracted from a data file for a certain condition, the average intensity of the baseline was determined and subtracted from each data point within the background subtracted file. This effectively corrects for the baseline DC offset of the HCl(v=1) emission profile. A straight horizontal baseline can be plotted before the emission profile by creating a column in the spreadsheet where two points (0,0 and first time point,0) are used to define the baseline trace. The nonlinear least-squares emission profile fits yield coefficients useful for determining the rate coefficients. The equation used to fit the profile is as follows:

$$f(t) = I_o(e^{-k_d t} - e^{-k_r t})$$

IGOR will require this form: $f(t) = Io * (\exp(-kd * t) - \exp(-kr * t))$

Where the coefficients are I_o, k_r, and k_d and the independent variable is t. The range to fit is from the point where the profile begins (time =0) to the last data point. The fit produces values for k_{rise} (k_r), k_{decay} (k_d), and I_o. These coefficients will be discussed in the next section.

IV. Results and Discussion

A. Determination of k_1 and k_v

The chain inhibited condition is controlled by using a chlorine atom precursor that cannot participate in a chain reaction with cyclohexane. Under such conditions the excited HCl fluorescence emission profile is dependent on the coefficients k_1 and k_v only. Since the chain is inhibited, the HCl(v) fluorescence rise is dependent on the rate coefficient, k_1, for the first propagation step, $Cl\cdot + RH \rightarrow HCl(v) + R\cdot$. The second propagation step doesn't occur. The fluorescence decay is due to vibrational relaxation (k_v).

Because of the common use of iodine monochloride (ICl) as a Cl* ($^2P_{1/2}$) precursor in our laboratory, initially experiments were conducted with 532 nm photolysis of ICl (with CCl_4 added to relax Cl*) to provide a chlorine atom without promoting a chain reaction. Unfortunately, these experiments did not provide data that led to reasonable values for k_1 and k_v. It may be that $R\cdot + ICl \rightarrow RI + Cl\cdot$ (or $R\cdot + ICl \rightarrow RCl + I\cdot$) is a complicating reaction in these experiments, but this was not pursued. Rather 266 nm photolysis of sulfur monochloride (S_2Cl_2) was used to provide Cl atoms in experiments to determine k_1 and k_v. Sulfur monochloride worked well for previous work in the Leone group, but it has a low vapor pressure and is somewhat messy to work with.

$$S_2Cl_2 + h\nu \xrightarrow{266nm} S_2Cl\cdot + Cl\cdot$$
$$Cl\cdot + RH \xrightarrow{k_1} HCl(v) + R\cdot$$
$$HCl(v) + M \xrightarrow{k_v} HCl + M$$

S_2Cl_2 was photolyzed by the fourth harmonic (266nm) from the Nd:YAG laser. The vapor pressure of S_2Cl_2 (~ 7 Torr) is insufficient backing pressure for the mass flow controllers so a mix of 4% S_2Cl_2 in argon was prepared to a final pressure of approximately 700 Torr. A 1% ratio had been successfully used in previous studies, but the linear flow rates necessary for reagent gas replenishment between laser shots (at least 10 cm/sec) were high enough for a 4% mix to be a safer option to prevent depletion of our stock. The concentrations of the reagents are approximately the same as in successful experiments on other chain systems and are presented in Table 2. The flow controllers were calibrated on the same day before experiments were conducted. The laser was adjusted to emit 4 milliJoule pulses at 266 nm to photolyze the S_2Cl_2. This selection provides acceptable [RH]/[Cl·] and [S_2Cl_2]/[Cl·] pseudo first order excesses without excessively promoting reagent exhaustion. The total pressure target was approximately 4.3 Torr. A representative HCl(v) fluorescence emission profile with a superimposed fit is shown in Figure 6.

Table 2 Concentrations used in the determination of k_1 and k_v.

	1	2	3	4	5	6	7
Argon [Ar](Torr)	4.3	4.3	4.3	4.3	4.3	4.3	4.3
Cyclohexane [RH](milliTorr)	10	15	20	25	30	35	40
[S_2Cl_2](milliTorr)	31	31	31	31	31	31	31

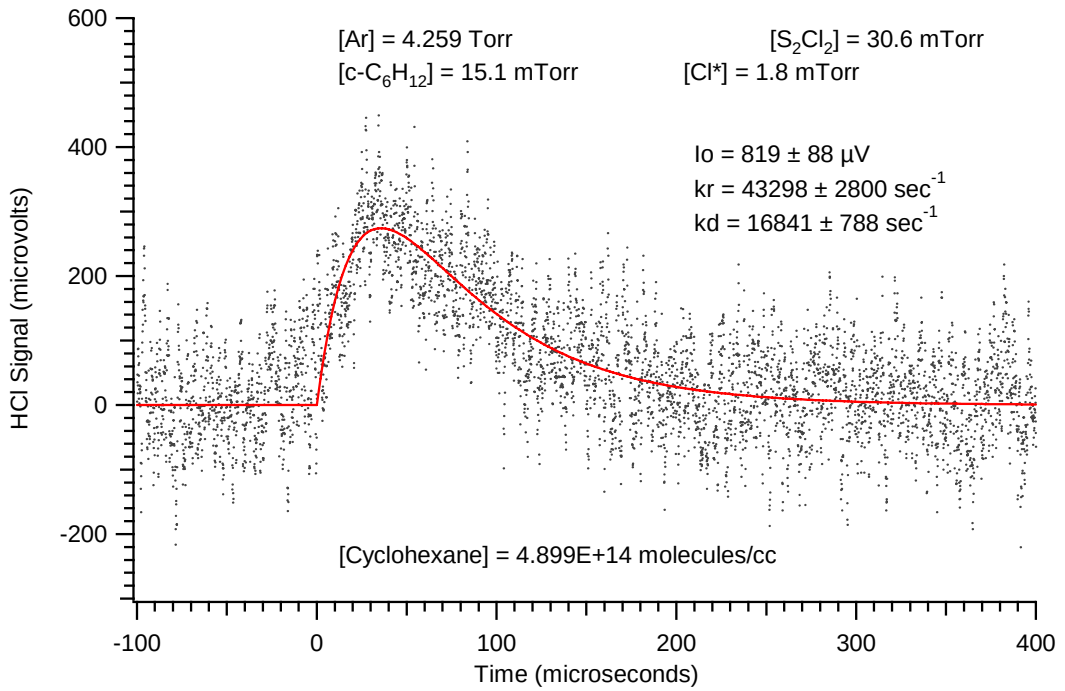

Figure 6: HCl(v) emission profile with rise due to k_1 and decay due to k_v.

As can be seen, the profiles were noisy, but they were adequate to yield good fits. A window coating began appearing where the laser beam passes through the quartz window. The windows were removed between experiments and cleaned with methanol to prevent this from interfering with the results. The coating chemical makeup and source are unknown.

In the "no chain" mechanism, $[HCl(v)]_t$ is given by:

$$[HCl(v)]_t = \frac{k_1'}{k_1' - k_v'}[Cl\cdot]_o (e^{-k_v' t} - e^{-k_1' t})$$

and the HCl(v) IR fluorescence profile follows the form:

$$I_f = I_o(e^{-k_{decay}t} - e^{-k_{rise}t})$$

The output parameters from fits of the fluorescence emission profiles are k_{rise}, k_{decay}, and I_o. Since $k_r = k_1$ [cyclohexane] and $k_d = k_v$ [cyclohexane], a plot of k_r or k_d versus cyclohexane concentration will be linear with a slope of k_1 or k_v respectively.

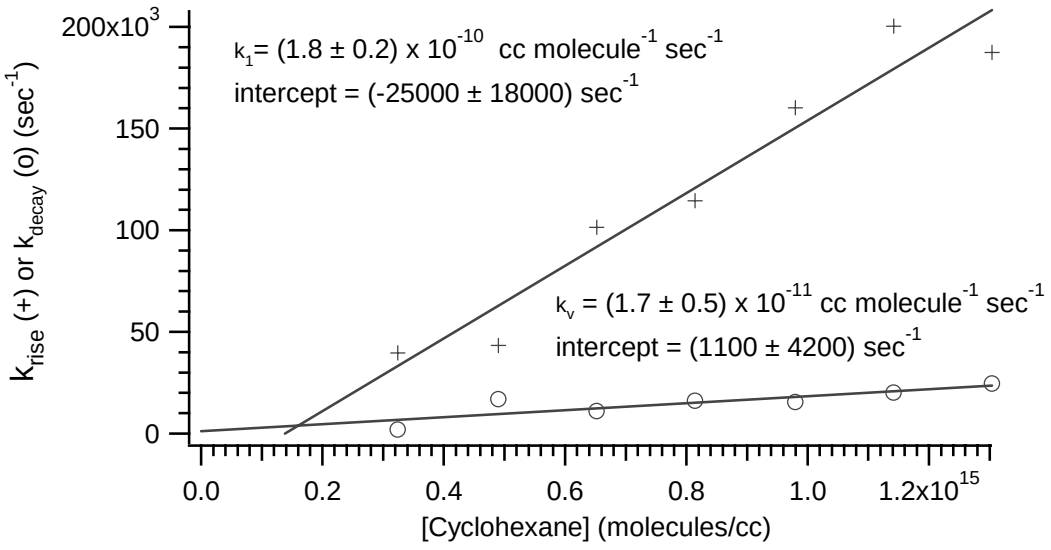

Figure 7: The linear plots to determine k_1 and k_v.

The values of the intercepts are of no consequence in the determination of k_1 and k_v, but they were expected to be near zero. Positive deviations in the k_1 plot would be attributed to diffusion out of the viewing region or reaction with a constant concentration impurity. Similarly small positive deviations in the k_v plot would be attributed to diffusion or relaxation by argon and chlorine (at constant concentrations). The uncertainties of the

intercepts are of the same order of magnitude as the values for the intercepts, and therefore the intercepts are considered to be approximately equal to zero. The value of k_1 was determined to be (1.8 ± 0.2) x 10^{-10} cc·molecule^{-1}·sec^{-1} and is in good agreement with the k_1 value of (2.0 ± 0.1) x 10^{-10} cc·molecule^{-1}·sec^{-1} reported by Davis et al[23]. The value of k_v was determined to be (1.7 ± 0.5) x 10^{-11} cc·molecule^{-1}·sec^{-1} which is comparable to the value of k_v reported by Nesbitt and Leone[8] for Cl_2/butane of (1.5 ± 0.2) x 10^{-11} cc·molecule^{-1}·sec^{-1}.

B. Determination of k_2

Recall that the equation for the concentration of HCl(v) in the unterminated Cl_2/RH chain reaction is:

$$[HCl(v)]_t = [HCl]_{ind}[e^{-k_v't} - e^{-(k_1'+k_2')t}] + \frac{k_{chain}}{k_v'}[1 - e^{-k_v't}] \qquad (51)$$

The first term of the equation describes a fast rise due to the exponent $k_1'+ k_2'$ and a subsequent decay due to the vibrational relaxation described by the k_v' exponent. The second term describes a rise to a steady state by the k_v' exponent. If we manipulate the experimental parameters (high $[Cl_2]$ / [RH]) to yield a HCl(v) emission profile where the first term is marginalized and contributes only a small induction feature at very early time on what is largely a rise to a steady-state profile, we have the advantage of fitting the rise to a steady-state after the initial induction feature to obtain the coefficient k_{chain} / k_v'. Under such conditions the equation for the concentration of HCl(v) is:

$$[HCl(v)]_t = \frac{k_{chain}}{k_v'}[1 - e^{-k_v' t}]$$

which correlates to the equation used to fit the fluorescence profile:

$$I_f = A[1 - e^{-k_v' t}]$$

Where:

$$A \propto \frac{k_{chain}}{k_v'}$$

and

$$k_{chain} \propto A k_v'$$

The fit yields values for A and k_v' used to calculate $k_{chain.}$ But also, from Eq. (53):

$$k_{chain} = \frac{k_1' k_2' [Cl\cdot]_o}{(k_1' + k_2')} \tag{53}$$

The scheme proposed by Nesbitt and Leone[4] for determining k_2 of the Cl_2/butane system was applied here for the Cl_2/cyclohexane system. If the substitution of the equation for

the chlorine radical concentration ($[Cl\cdot]_o \propto [Cl_2]E_{laser}$) is made and the prime shorthand used to denote pseudo first order rate coefficients is abandoned, the equation becomes:

$$k_{chain} \propto \frac{k_1[RH]k_2[Cl_2]([Cl_2]E_{laser})}{k_1[RH]+k_2[Cl_2]}$$

We can rearrange this equation to a more useful form:

$$\frac{[RH][Cl_2]E_{laser}}{k_{chain}} \propto \frac{1}{k_2}\frac{[RH]}{[Cl_2]}+\frac{1}{k_1}$$

It's clear that a plot of $\frac{[RH][Cl_2]E_{laser}}{k_{chain}}$ versus $\frac{[RH]}{[Cl_2]}$ for a series of cyclohexane concentrations will be linear with a slope of $\frac{1}{k_2}$ and an intercept of $\frac{1}{k_1}$. Simply dividing the slope by the intercept yields the ratio of $\frac{k_1}{k_2}$. Since k_1 has already been determined, this ratio can be used to produce a value for k_2.

Initially simulations were done with the simple Excel simulator to help decide the reagent concentrations for these experiments. The result is shown in Figure 8 for $[Cl_2]/[RH] = 80$. This profile marginalizes the $[HCl]_{ind}$ term and emphasizes the k_v' rise to steady-state, but reveals nothing about the reality of reagent exhaustion due to the chain reaction. The GEAR simulation in Figure 9 provides a more accurate picture of this reality for the conditions indicated on the plot.

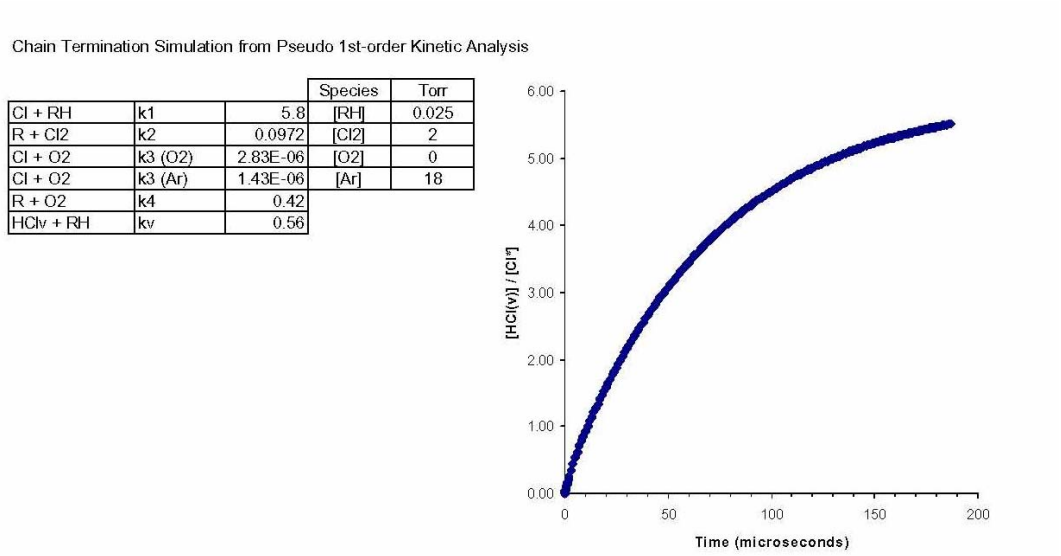

Figure 8: The Excel simulator: the early rise portion due to $[HCl]_{ind}$ in Eq.(51) is minimized.

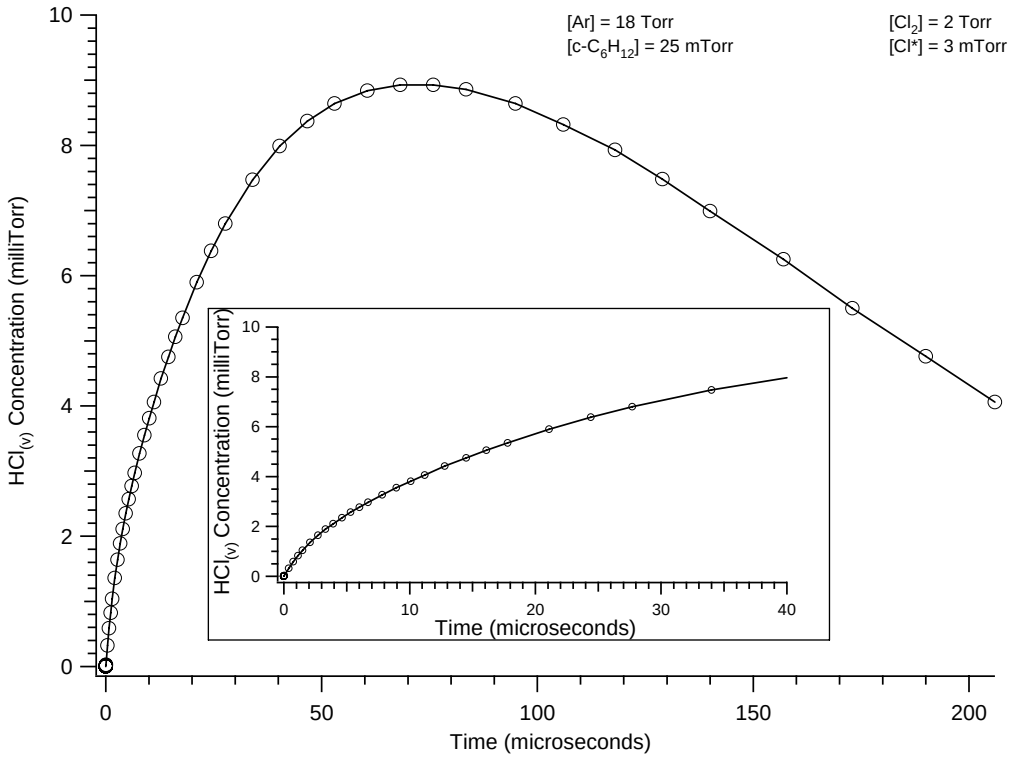

Figure 9: A GEAR simulation: the early rise portion due to $[HCl]_{ind}$ in Eq.(51) is minimized.

The simulations were performed using the reagent concentrations of Table 3 and 3 milliTorr chlorine atom concentration which should be suitable to determine k_2. The undesirable decay due to reagent exhaustion evident in Figure 9 indicates that the equation used to fit the profile must include an additional decay term. The equation used to fit the profile is:

$$I_f = A(e^{-k_d t} - e^{-k_r t})$$

where $k_v' = k_r$ from the signal rise and the k_d term allows for decay due to reagent exhaustion.

Table 3 Reagent concentrations used in the determination of k_2

	1	2	3	4	5
Argon [Ar](Torr)	18	18	18	18	18
Cyclohexane [RH](milliTorr)	49	74	98	123	147
Chlorine [Cl_2](Torr)	2	2	2	2	2

A series of experiments to determine k_2 were conducted with conditions in Table 3. The laser energy was adjusted for 2 milliJoules at 355nm which produces 3 milliTorr of chlorine atoms. The reagent concentrations in Table 3 along with the stated laser energy yields the appropriate HCl(v) emission profile needed to determine k_2 while simultaneously maintaining linear flow rates of at least 10 cm/sec and pseudo first-order excesses [RH]/[Cl·] and [Cl_2]/[Cl·] of at least 10 to 1.

The data were collected as a 5000 shot summed average. One of the collected profiles with a superimposed fit is shown in Figure 10.

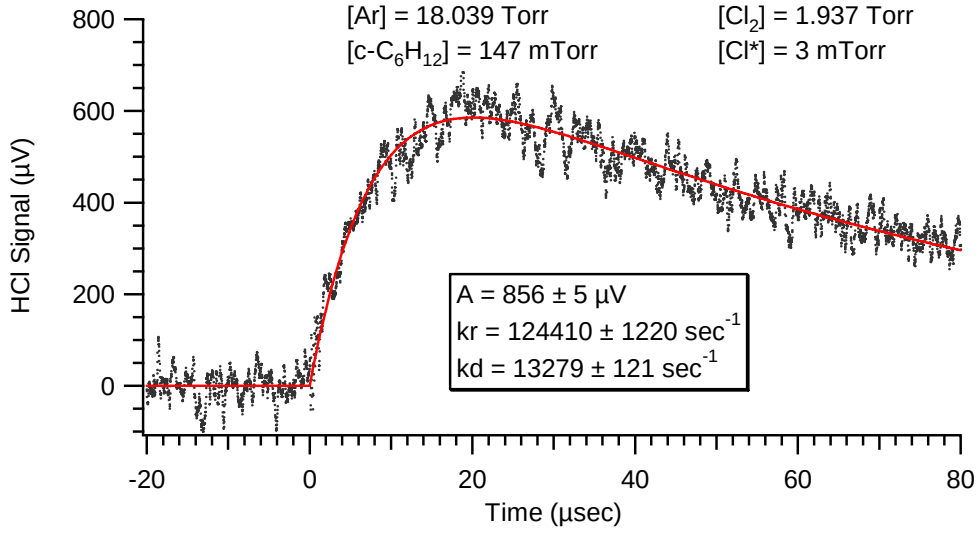

Figure 10: $HCl_{(v)}$ emission profile: the early rise portion due to $[HCl]_{ind}$ in Eq. (51) is minimized.

The subsequent linear plot is as below:

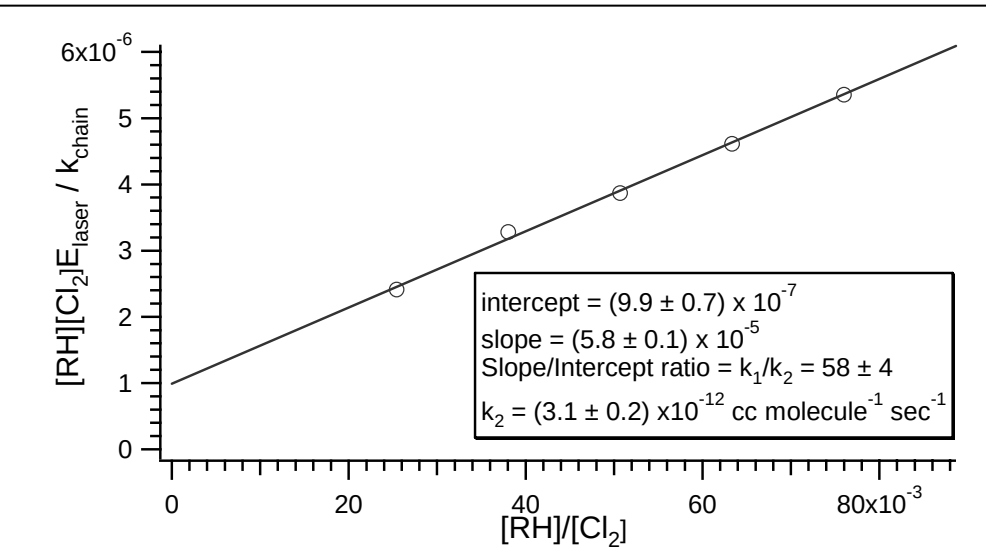

Figure 11: The linear plot yielding the k_1/k_2 ratio.

As seen from the inset of the linear plot, our k_1/k_2 ratio is approximately 58 ± 4. The k_2 value calculated from this ratio is (3.1 ± 0.2) x 10^{-12} cc·molecule^{-1}·sec^{-1} using the k_1 value ((1.8 ± 0.2) x 10^{-10} cc·molecule^{-1}·sec^{-1}) determined in this study. Using a hard-sphere k_1 value of 3 x 10^{-10} cc·molecule^{-1}·sec^{-1} would increase k_2 to 5.2 x 10^{-12} cc·molecule^{-1}·sec^{-1}. This larger k_2 value compares more favorably with the value of (6.8 ± 1.5) x 10^{-12} cc·molecule^{-1}·sec^{-1} for the reaction of butyl radicals with Cl_2 in Nesbitt and Leone's study of the Cl_2/ butane chain reaction[8].

C. The Termination Rate Coefficient k_4

It has been previously reported by Klingshirn and Dolson[11] that it may also be possible to determine the termination rate coefficients from observations of the HCl(v) emission profiles. Recall the termination processes with added O_2 from section IB:

$$Cl\cdot + O_2 + M \xrightarrow{k_3} ClO_2\cdot + M$$
$$R\cdot + O_2 \xrightarrow{k_4} RO_2\cdot$$

It was previously established in this thesis that the radical chain termination rate would be dominated by k_4 because of the necessity of a third body for the removal of the chlorine atom by k_3.

Recall Eqs. (77)-(79) for the chain with an added radical scavenger:

$$\frac{[HCl(v)]_t}{[Cl\cdot]_o} = Ae^{-\lambda_+ t} + Be^{-\lambda_- t} - (A+B)e^{-k_v' t} \qquad (77)$$

$$A = \frac{k_1'(k_1' + k_3' - \lambda_-)}{(\lambda_+ - \lambda_-)(k_v' - \lambda_+)} \qquad (78)$$

$$B = \frac{k_1'(\lambda_+ - k_1' - k_3')}{(\lambda_+ - \lambda_-)(k_v' - \lambda_-)} \qquad (79)$$

When $k_1' + k_2' >> k_3' + k_4'$ it can be shown that λ_+ and λ_- have simple approximate expressions:

$$\lambda_+ \approx k_1' + k_2'$$
$$\lambda_- \approx k_3' + k_4' \approx k_4' = k_4[O_2]$$

We can show that $\lambda_+ > k_v' > \lambda_-$ when our oxygen concentrations are low, therefore we can see that the A coefficient will be negative because of the $(k_v' - \lambda_+)$ factor in the denominator of Eq. (78). This means that the first term in Eq. (77) describes a rapid rise at early time. The term with k_v' in the exponent describes either a rise or a decay at intermediate time depending on whether A or B has the larger magnitude. The B coefficient will be positive so that the second term in Eq. (77) describes the chain termination decay at late time. Exponential fits of these late decays should yield values for λ_- or, as I called them in the fitting equation, k_{decay} for a series of oxygen concentrations. A plot of the values for λ_- in units of sec^{-1} versus the oxygen concentrations in units of $molecule \cdot cc^{-1}$ should be linear with a slope of k_4 in units of $cc \cdot molecule^{-1} \cdot sec^{-1}$.

A HCl(v) emission profile that rises to a steady state in the absence of a chain terminating species (no oxygen) is an ideal starting condition from which to study the chain termination effects of an added radical scavenger. The concentrations in the first column of Table 4 are displayed in the plot of the Excel simulation of Figure 12. Though the profile has a fast rise at early time and then a decay at intermediate time to a steady-

state, these concentrations were determined to achieve a reasonable profile from which to begin the study of the effects of radical scavenging.

Table 4 Concentrations used to perform the GEAR termination simulation.

	1	2	3	4
Argon [Ar](Torr)	18	18	18	18
Cyclohexane [RH](milliTorr)	0.17	0.17	0.17	0.17
Oxygen [O_2] (milliTorr)	0	10	25	50
Chlorine [Cl_2](Torr)	0.68	0.68	0.68	0.68

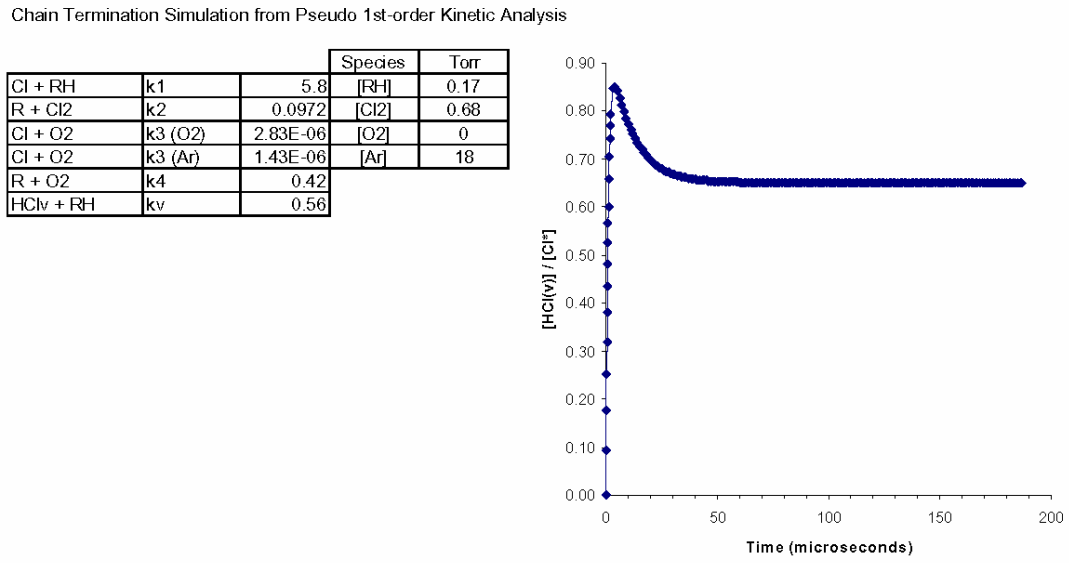

Figure 12: The Excel simulation using pressures from the first column of Table 4.

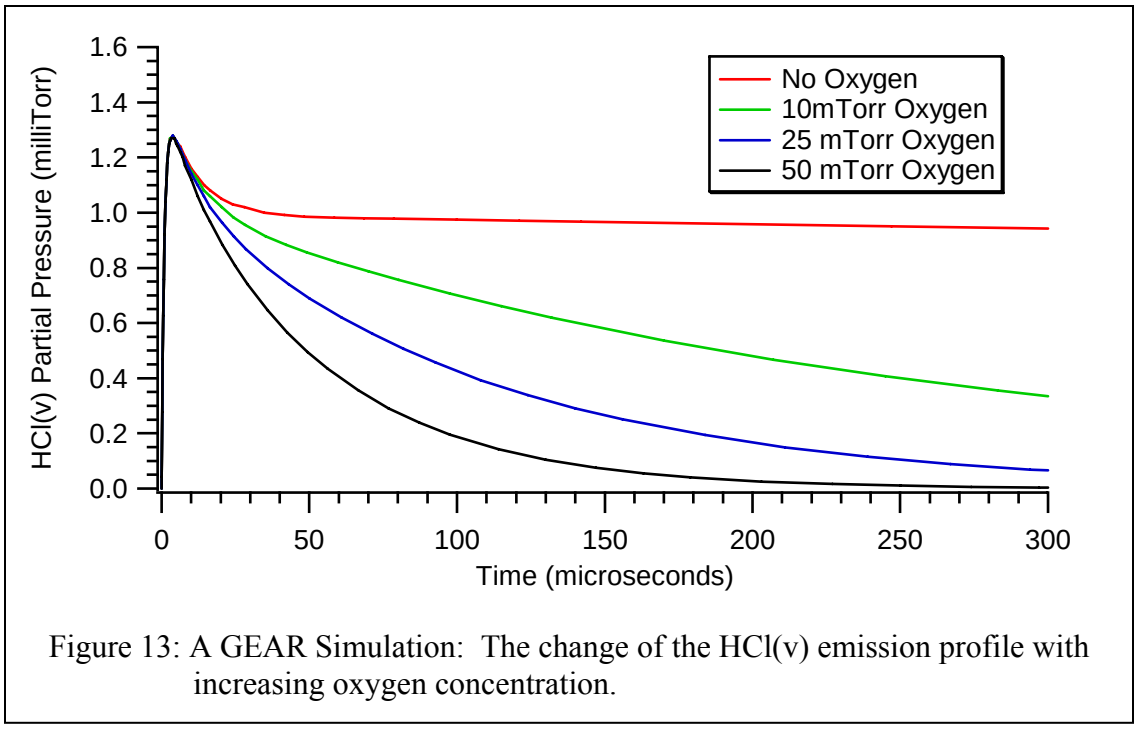

Figure 13: A GEAR Simulation: The change of the HCl(v) emission profile with increasing oxygen concentration.

Figure 13 is the result of a GEAR simulation of the terminated chain reaction using concentrations from Table 4 and demonstrates the effect on the emission profile of adding oxygen in increments of 10, 25, and 50 milliTorr. The first simulation at the revised concentrations and using a chlorine atom concentration of 3 milliTorr revealed more reagent exhaustion than was hoped so the concentration of chlorine atom was reduced to 1.5 milliTorr to produce the simulated plot shown in Figure 13. The effects of reagent exhaustion manifest as a decay of the steady-state (late time) portion of the profile for the no oxygen condition. On this time scale the contribution due to reagent exhaustion appears to be negligible.

A plot of the simulated HCl(v) fluorescence profile for each oxygen addition with the superimposed fit and values for λ_{-} (k_{decay}) follow in Figures 14, 15, and 16.

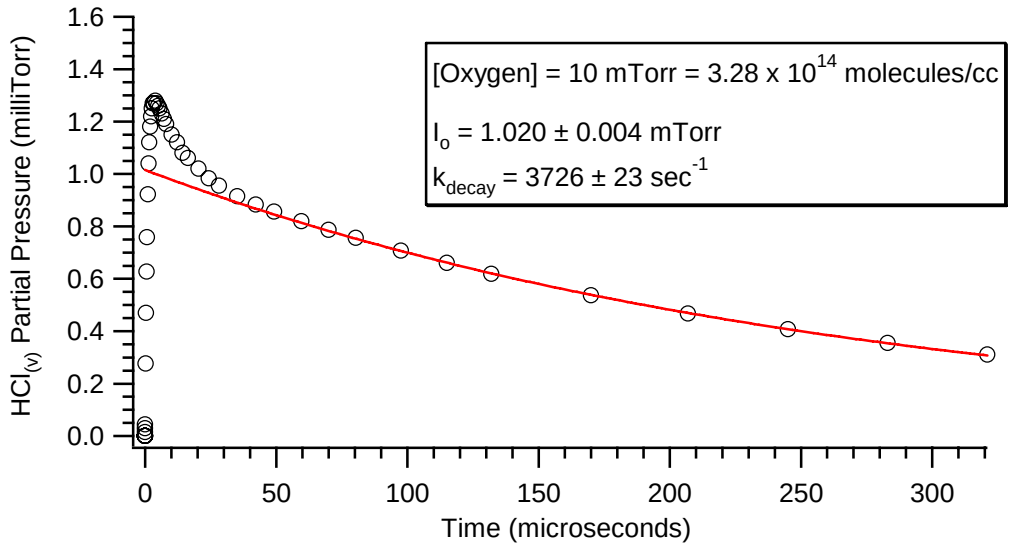

Figure 14: Simulated data for 10 milliTorr oxygen addition.

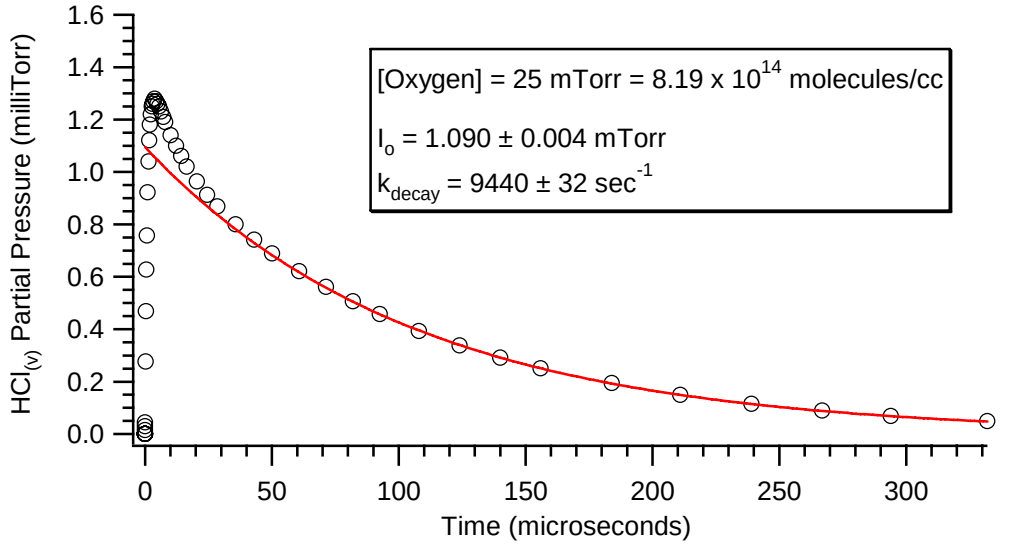

Figure 15: Simulated data for 25 milliTorr oxygen addition.

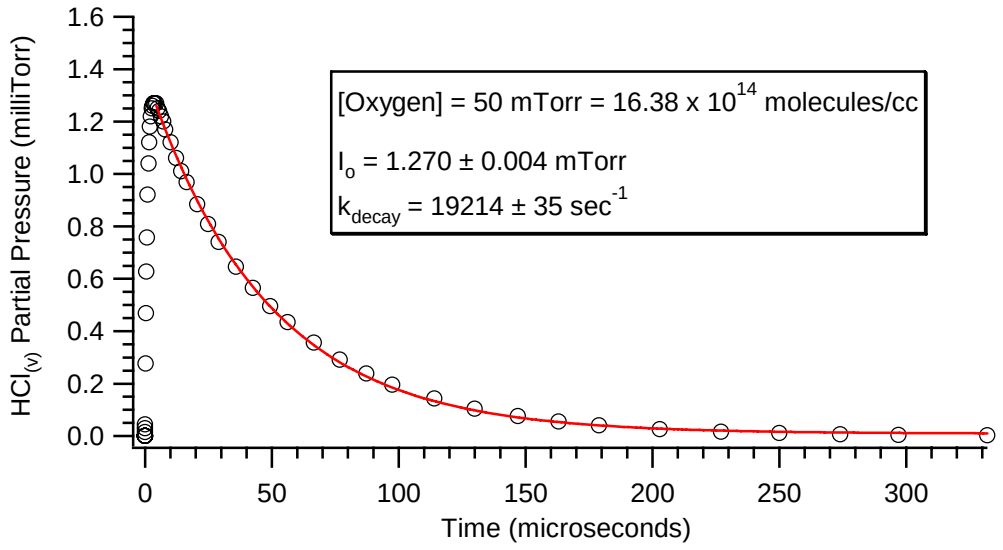

Figure 16: Simulated data for 50 milliTorr oxygen addition.

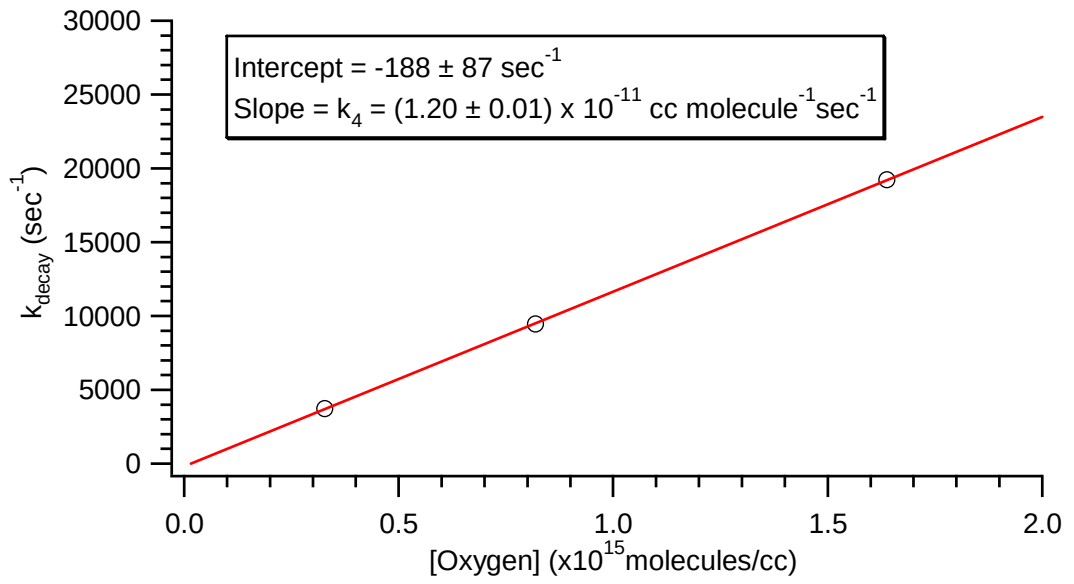

Figure 17: The k_{decay} vs. [Oxygen] plot for the simulated data.

A plot of the k_{decay} values from the fits of Figures 14-16 versus the oxygen concentration is very linear as seen in Figure 17 and the slope yields a simulation k_4 value of (1.20 ± 0.01) x 10^{-11} cc·molecule^{-1}·sec^{-1}. This value is quite a reasonable approximation of the literature value for k_4 ((1.3 ± 0.2) x 10^{-11} cc·molecule^{-1}·sec^{-1}) from the work of Platz et al.[16] used to generate the GEAR simulations that yielded Figures 14-16. The intercept is approximately zero given the uncertainty of the plot. These results gave rather compelling evidence of the plausibility of determining the termination coefficient k_4 from experimental data.

Experiments for k_4 determination were performed using the concentrations in Table 5, but they produced rather curious results. The HCl (v) emission profiles in these experiments were predicted to (Figure 13) have a fast rise and then a decay at intermediate time to a steady-state level if $[O_2] = 0$ or to a second decay due to O_2 termination. The profile, as shown in Figure 18, appears to have a fast rise and then a slower second rise at intermediate time rather than the predicted decay. This feature is subtle given the signal-to-noise ratio, but the second rise was unexpected based on the simulation and looked suspiciously like a scenario where the exponential k_v' term

Table 5 Concentrations used in the first experiments to determine k_4

	1	2	3	4	5	6	7
Argon [Ar](Torr)	3.822	3.822	3.822	3.822	3.822	3.822	3.822
Cyclohexane [RH](milliTorr)	174	174	174	174	174	174	174
Oxygen [O_2] (milliTorr)	0	42	85	128	171	214	257
Chlorine Atom [Cl*] (milliTorr)	3.8	3.8	3.8	3.8	3.8	3.8	3.8
Chlorine [Cl_2](milliTorr)	704	704	704	704	704	704	704

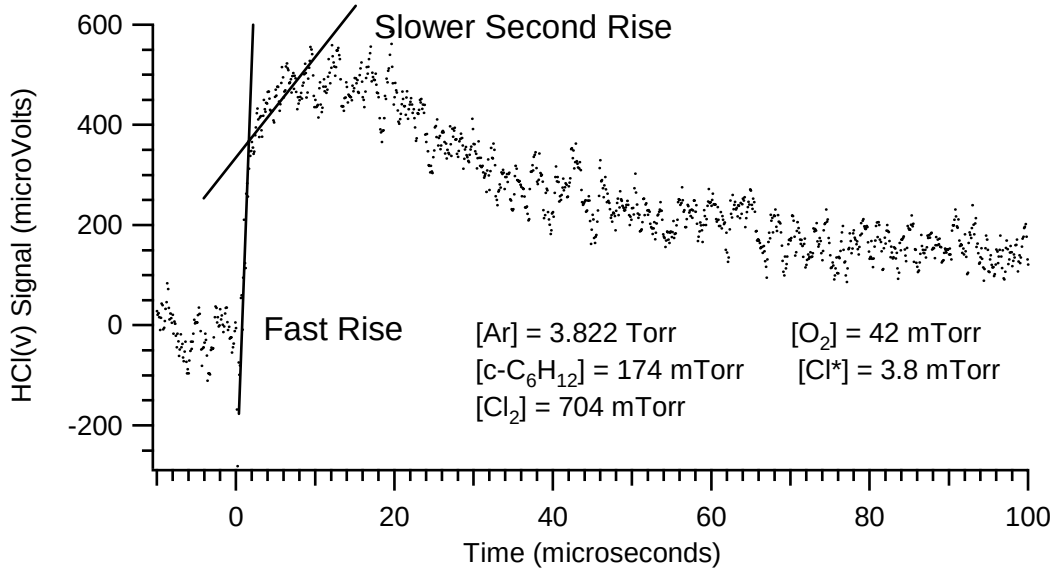

Figure 18: The appearance of an unexpected second rise at intermediate time.

in Eq. (77) describes a second rise at intermediate time. The simulated data used to develop Figure 13 was based on the k_2 value determined previously in this work, (3.1 ± 0.2) x 10^{-12} cc·molecule^{-1}·sec^{-1}, which yielded a "no oxygen" simulated HCl(v) profile with a fast rise at early time followed by a decay at intermediate time to a steady-state. When Nesbitt and Leone's[8] rate coefficient for the butyl + Cl_2 reaction of (6.8 ± 1.5) x 10^{-12} cc·molecule^{-1}·sec^{-1} is substituted for k_2 in the Excel and GEAR simulations, the decay at intermediate time in Figure 12 becomes a second rise as observed in Figures 19-22. These findings provide support for a larger k_2 value for the cyclohexyl + Cl_2 reaction. While the k_2 value reported earlier in this thesis may be in some doubt, k_4 determinations are to be obtained from the longer time decay of the steady-state fluorescence. These observations are unaffected by the k_1 or k_2 values.

Chain Termination Simulation from Pseudo 1st-order Kinetic Analysis

			Species	Torr
Cl + RH	k1	5.8	[RH]	0.17
R + Cl2	k2	0.2203	[Cl2]	0.68
Cl + O2	k3 (O2)	2.83E-06	[O2]	0
Cl + O2	k3 (Ar)	1.43E-06	[Ar]	4
R + O2	k4	0.42		
HClv + RH	kv	0.56		

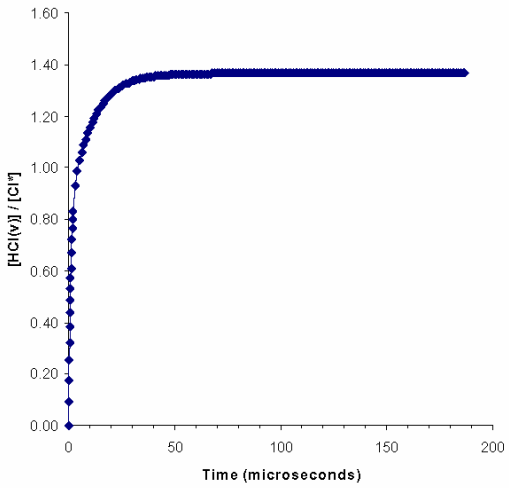

Figure 19: The Excel simulation using the k_2 value for the butyl + Cl_2 reaction and no oxygen .

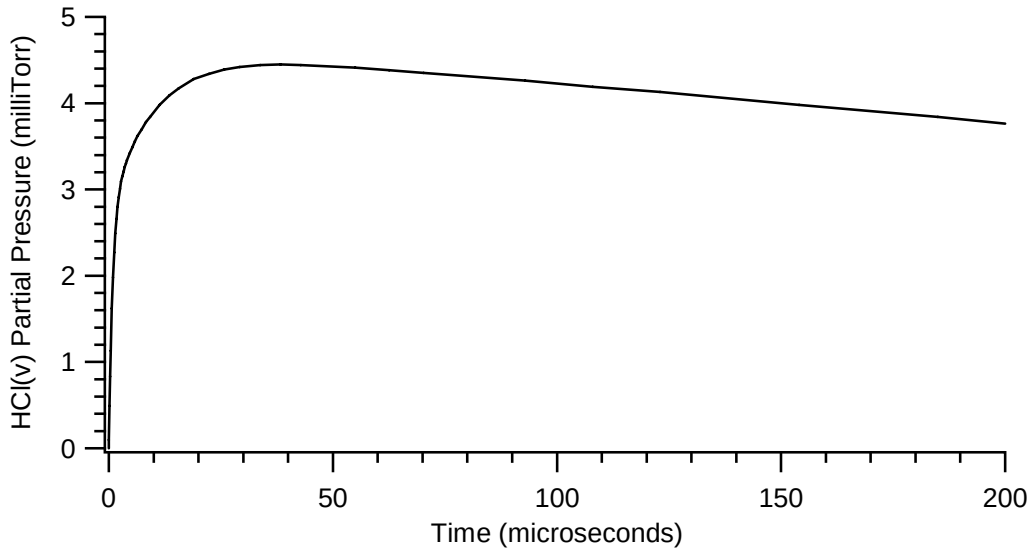

Figure 20: The HCl(v) profile from the GEAR simulation with no oxygen. Some loss of steady-state signal is due to reagent exhaustion in the chain reaction.

Chain Termination Simulation from Pseudo 1st-order Kinetic Analysis

			Species	Torr
Cl + RH	k1	5.8	[RH]	0.17
R + Cl2	k2	0.2203	[Cl2]	0.68
Cl + O2	k3 (O2)	2.83E-06	[O2]	0.01
Cl + O2	k3 (Ar)	1.43E-06	[Ar]	4
R + O2	k4	0.42		
HClv + RH	kv	0.56		

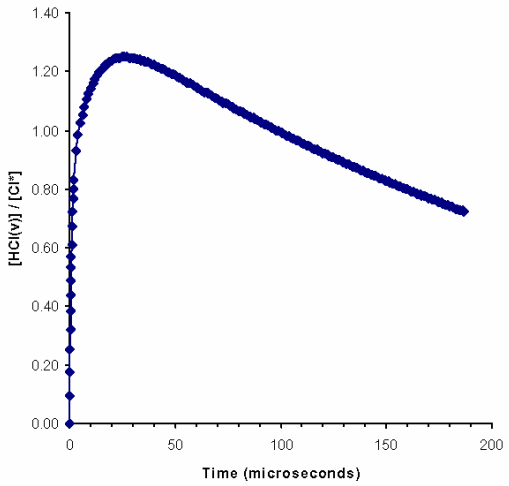

Figure 21: The Excel simulation using the k_2 for the butyl + Cl_2 reaction and [O_2] = 10 milliTorr.

The HCl(v) fluorescence profiles with added oxygen also were simulated with the higher k_2 value. In both simulations, presented in Figure 21 and 22, an early fast rise is followed by a second slower rise at intermediate time. Both simulations exhibit the expected O_2-terminated decays.

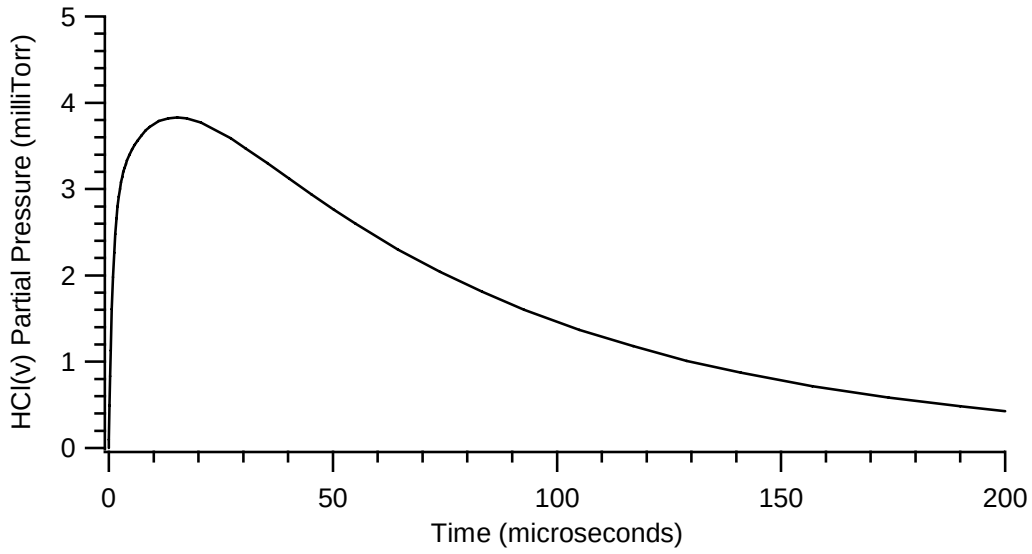

Figure 22: The HCl(v) profile from the GEAR simulation [O_2] = 37 mTorr.

Experiments to determine k_4 were performed with the partial pressures stated in Table 5. The profile without oxygen is shown in Figure 23. Figures 24 and 25 display the fluorescence profile at the smallest and the largest concentrations of oxygen added,

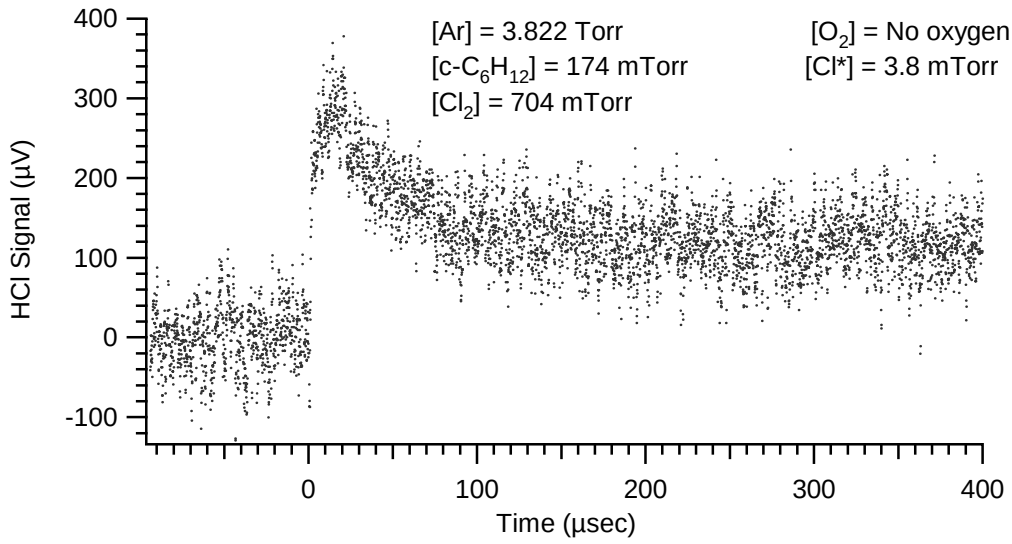

Figure 23: The fluorescence profile collected experimentally without oxygen and using the concentrations displayed in the first column of Table 5.

respectively. Several of the signal decays in these observations exhibited a fast decay and an unexpected slower decay component. The fast decays were fit to an exponential function to determine k_{decay} for each oxygen concentration. A kinetic plot of this data is presented in Figure 26. The slower decays did not depend upon $[O_2]$ in a consistent fashion.

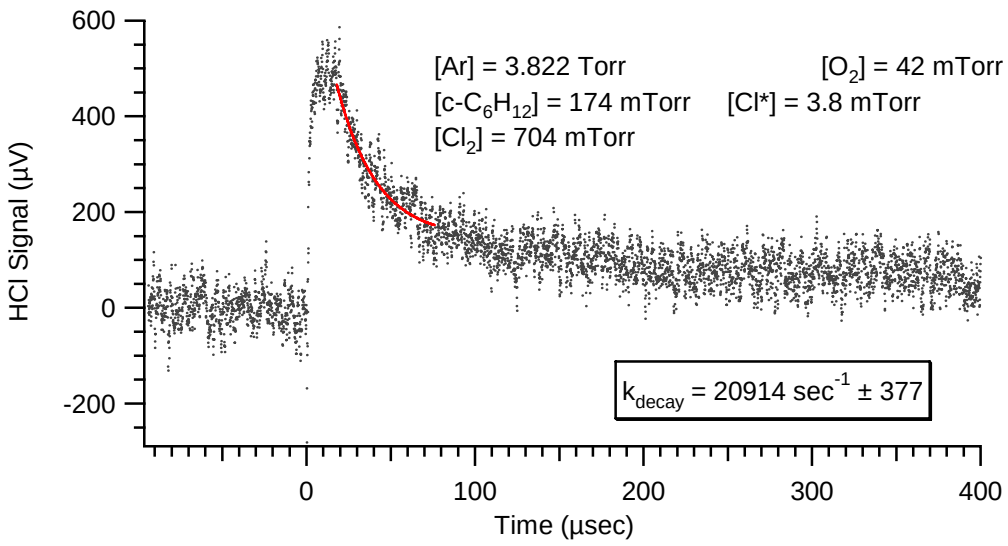

Figure 24: The profile collected experimentally with $[O_2]$ = 42 mTorr

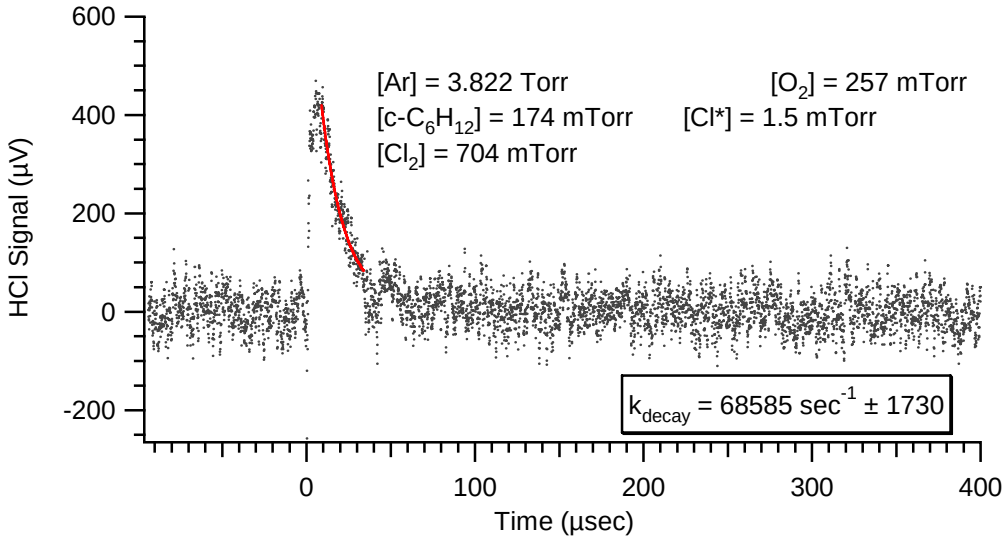

Figure 25: The profile collected experimentally with $[O_2]$ = 257 mTorr

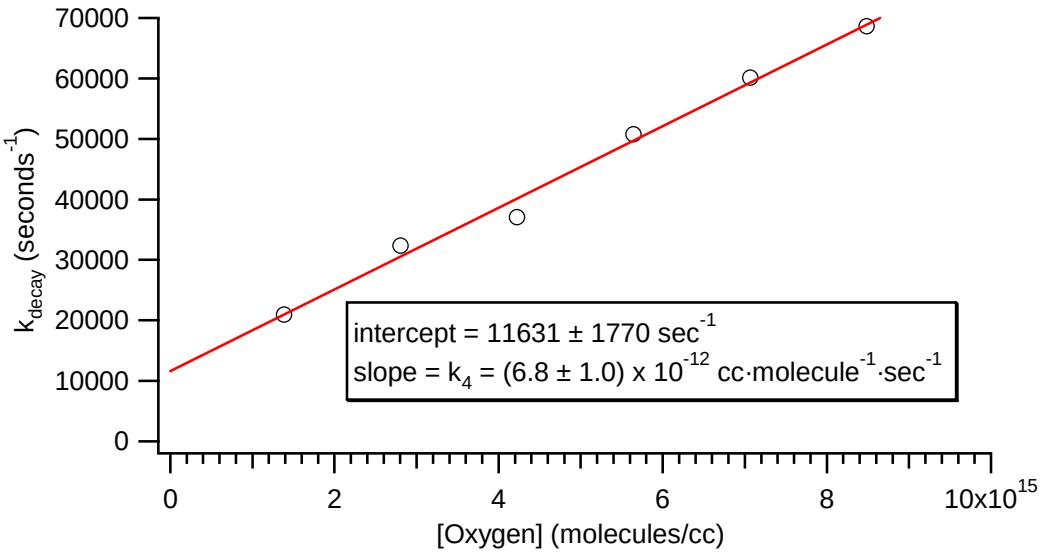

Figure 26: The linear plot of k_{decay} vs. $[O_2]$ to determine k_4 from the slope.

The experimentally determined value for k_4 displayed in Figure 26, (6.8 ± 1) x 10^{-12} cc·molecule^{-1}·sec^{-1}, was lower than the value reported by Platz et al.[16] of (1.3 ± 0.2) x10^{-11} cc·molecule^{-1}·sec^{-1}and the value reported by Wu and Bayes[24] of (1.4 ± 0.2) x 10^{-11} cc·molecule^{-1}·sec^{-1}. The linear fit produces a value for the y-intercept that is approximately zero within twice the stated uncertainty. The odd appearance of the profile was still troubling.

There is suspicion that these experimental parameters may be closer to the "hot chain" regime than previously thought (The hot chain will be commented on later in this thesis). It was hoped that again running the experiment with five times the concentration of argon than previously employed would provide a larger thermal sink and thus inhibit the onset of the "hot chain" regime.

Figure 27 shows a comparison of two HCl(v) fluorescence profiles when the argon concentration is increased five fold while holding all other experimental parameters constant. The argon concentration has been increased to prevent the chain reaction from developing into a thermally driven chain reaction and should have no effect on the profile otherwise. Figure 27 shows that the HCl(v) fluorescence signal decays to the baseline when the higher argon pressure is used. This seems to confirm the earlier influence of the "hot chain" reaction on the decay rate measurements in the previous k_4 experiments (Table 5 and Figures 23-26). Further, it suggests that a repeat of these experiments, but with an argon partial pressure nearer to 23 Torr, should obtain a greater success in determining k_4.

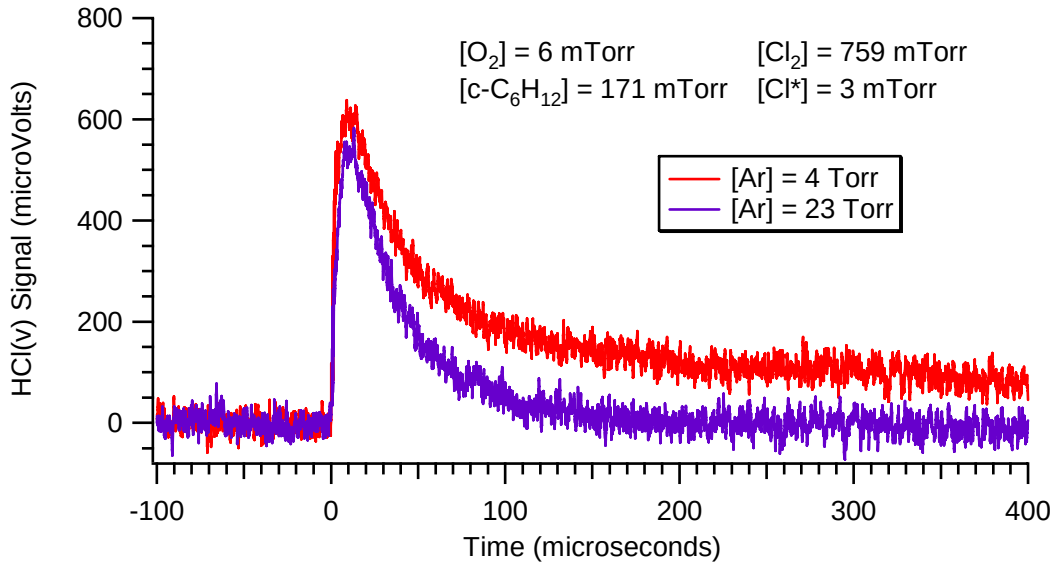

Figure 27: The effect of increasing the argon concentration by a factor of five.

These suggested experiments were done with 22.57 Torr of argon and with the other concentrations as presented in Table 6. The fluorescence profiles are presented in Figure 28 for the low end of oxygen concentration and in Figure 29 for the high end of oxygen concentration. Even though the thermally driven chain is suppressed with the higher argon pressure, the HCl(v) signal decays in these experiments are best fit by a

Table 6 Concentrations used in the experiments to determine k_4 with 5 times more argon.

	1	2	3	4	5	6
Argon [Ar](Torr)	22.57	22.57	22.57	22.57	22.57	22.57
Cyclohexane [RH](milliTorr)	171	171	171	171	171	171
Oxygen [O_2] (milliTorr)	0	6	20	48	76	104
Chlorine Atom [Cl*] (milliTorr)	3.1	3.1	3.1	3.1	3.1	3.1
Chlorine [Cl_2](milliTorr)	759	759	759	759	759	759

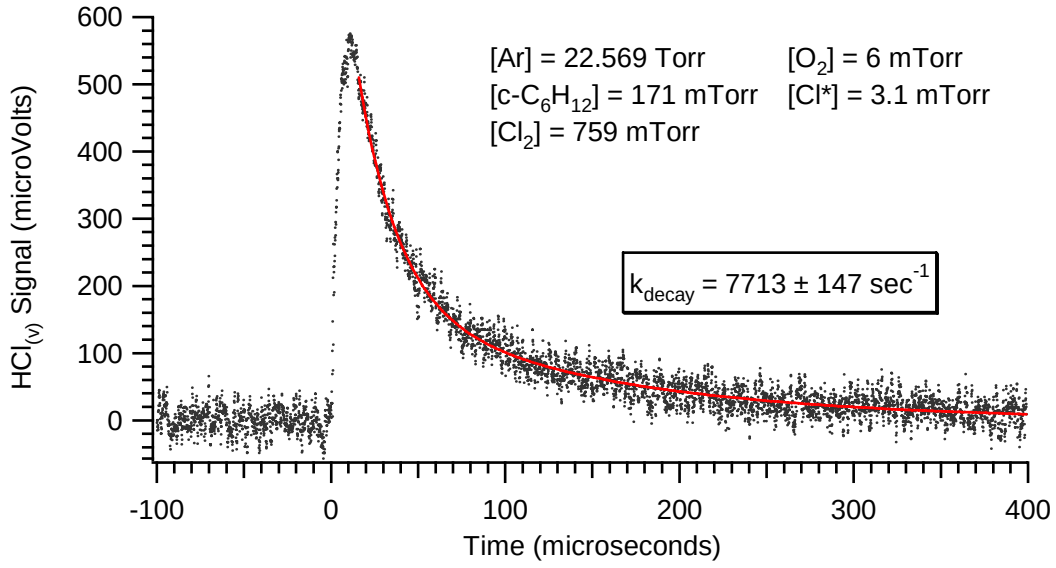

Figure 28: The profile with increased argon at the low end of oxygen concentration.

double exponential decay function – except that the highest [O_2] experiment (Figure 29) is best fit by a single exponential decay.

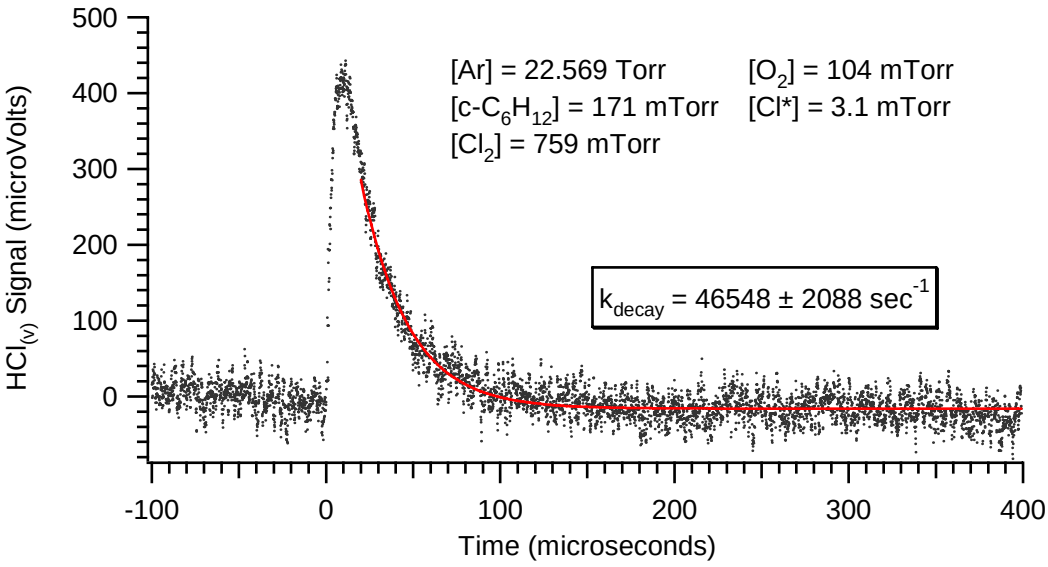

Figure 29: The profile with increased argon at the high end of oxygen concentration.

The faster decay rate has no simple dependence upon [O_2]; it rises at first and then falls with increasing [O_2], and there is only a single decay at the highest [O_2] = 0.104 Torr in these experiments. Recall that the kinetic analysis of the O_2-terminated chain reaction predicts a single exponential decay of the HCl(v) fluorescence. The best explanation for the unexpected additional decay without a sensible [O_2] dependence seems to be that the cyclohexyl radical chain carriers may undergo a second-order addition or disproportionation reaction at the concentrations generated in these experiments. Such a reaction would result in a self-termination of the chain reaction in the absence of oxygen addition. The oxygen termination step would then be in competition with the self-termination process. The single exponential decay observed at 0.104 Torr O_2 may signal the point at which the O_2 termination becomes the dominant

termination process. GEAR simulations, presented later, support this explanation for the faster HCl(v) fluorescence decay rates observed in these experiments.

The slower HCl(v) fluorescence decay rate in these experiments has a linear dependence upon $[O_2]$ and is plotted in Figure 30 along with an unweighted linear least squares fit of the five points. The single exponential decay rate for the 0.104 Torr O_2 experiment falls nicely on this line and is included in the fit.

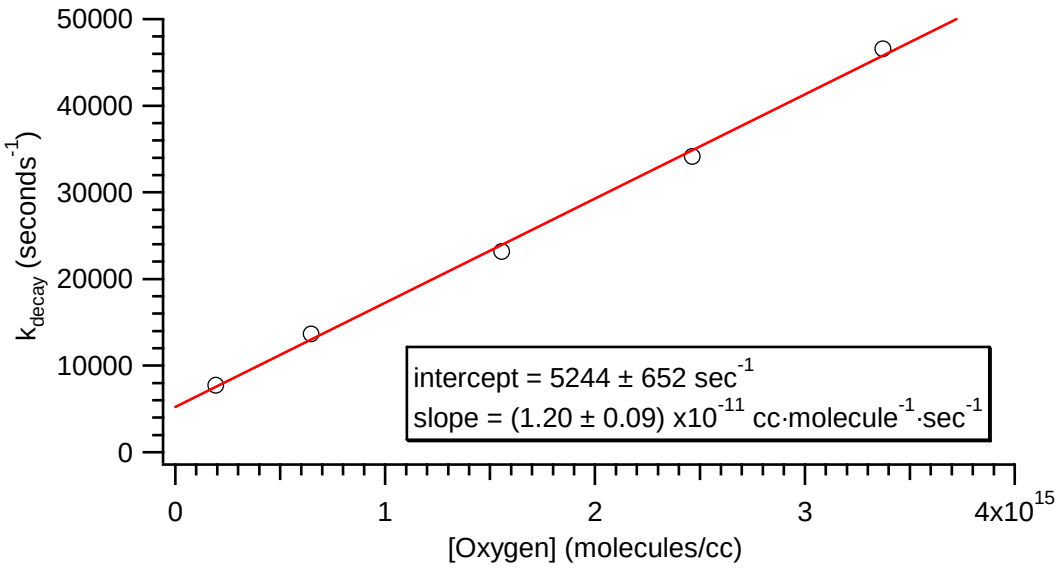

Figure 30: The linear plot to determine k_4 at the higher argon concentration.

The slope of the plot in Figure 30 yields a k_4 value of (1.20 ± 0.09) x 10^{-11} cc·molecule^{-1}·sec^{-1}, which is identical to the result predicted from the GEAR simulations of Figure 17. This k_4 value is in very good agreement with two previous experimental measurements[16,24] of the rate coefficient for the addition reaction of cyclohexyl radicals with molecular oxygen. Platz et al.[16] generated cyclohexyl radicals, in gas mixtures containing O_2, in a pulsed radiolysis experiment via the reaction of F· atoms with

cyclohexane. They monitored the 1-4 μs transient absorption signals at 280 nm as an indication of $RO_2\cdot$ formation and determined a rate coefficient of (1.3±0.2) x 10^{-11} cc·molecule^{-1}·sec^{-1}. Wu and Bayes[24] prepared cyclohexyl radicals from the 193 nm photolysis of CCl_4 and subsequent reaction of Cl· atoms with cyclohexane. They monitored the loss rates of cyclohexyl radicals in the presence of O_2 with mass spectrometry and determined a rate coefficient of (1.4±0.2) x 10^{-11} cc·molecule^{-1}·sec^{-1}.

D. Summary and Concluding Remarks

Table 7 summarizes the rate coefficients obtained by the laser photolysis/ infrared chemiluminescence detection technique for the O_2-terminated Cl_2/cyclohexane chain reaction studied in this thesis. The k_1 value determined in this work is in excellent agreement with the more direct study of Davis et al.[23] in a flash photolysis/resonance fluorescence study of the reaction. Their method of direct observations of Cl· atoms in real time yields absolute rate coefficients. The k_1 value determined here also is in reasonable agreement with a series of four relative rate coefficients, (2.4 to 3.6) x 10^{-10} cc·molecule^{-1}·sec^{-1}, found in the NIST Chemical Kinetics database.[25] Most of the relative rate studies use gas chromatographic analysis of product appearance rates or reactant disappearance rates in competitive chlorination experiments with another organic compound , the standard, for which the rate coefficient is thought to be well determined. The rate coefficients for these experiments seem to be systematically high relative to the absolute rate study of Davis et al.[23] For comparison, it is noted that a typical bimolecular Cl· + RH hard-sphere rate coefficient at 300K is near 3 x 10^{-10} cc·molecule^{-1}·sec^{-1} so that

Table 7: A summary of the rate coefficients determined in this study by the laser photolysis/infrared chemiluminescence technique*.

Reaction	k_i	This Work	Literature
$Cl\cdot + RH \rightarrow HCl(v = 0, 1) + R\cdot$	k_1	18 ± 2	20 ± 2 [23]
$R\cdot + Cl_2 \rightarrow RCl + Cl\cdot$	k_2	0.31 ± 0.02	none
$HCl(v=1) + RH \rightarrow HCl(v=0) + RH(v)$	k_v	1.7 ± 0.5	none
$R\cdot + O_2 \rightarrow RO_2$	k_4	1.2 ± 0.3	1.3 ± 0.2 [16] 1.4 ± 0.2 [24]

* The rate coefficients are in units of 10^{-11} cc/molecule·sec.

all of these experimental k_1 values represent a relatively efficient reaction of Cl· atoms with cyclohexane. This suggests that reaction, $Cl\cdot + c\text{-}C_6H_{12} \rightarrow HCl + c\text{-}C_6H_{11}\cdot$, has a low activation barrier and few steric restrictions.

The k_2 value determined in this work seems secure from the quality of the plot in Figure 11; however, it has been noted already that a higher k_2 value would appear to fit the observation of the second rise feature in Figure 18. Simulations in Figs. 19 and 20 using $k_2 = 6.8 \times 10^{-12}$ cc·molecule^{-1}·sec^{-1} (the k_2 value for the somewhat similar butyl + Cl_2 reaction[8]) reproduce the second rise in Figure 18 fairly well. Additional evidence argues for an even higher value. Tyndall et al.[26] have determined the ratio of rate coefficients for sec-butyl radicals with Cl_2 relative to that with O_2 to be 3.1 ± 0.4. An argument may be made that because the cyclohexyl radical also is a secondary alkyl radical and because at least some of the cyclohexyl + diatomic collision geometries are not very different from that for the sec-butyl radical, a similar ratio of rate coefficients

might apply to the k_2/k_4 ratio for cyclohexyl + Cl_2 and cyclohexyl + O_2. This argument would predict $k_2 = 3.1\ k_4 = 3.7 \times 10^{-11}$ cc·molecule^{-1}·sec^{-1}, which is twelve times higher than the k_2 determined in this work. A similar argument, applied to the butyl + Cl_2 rate coefficient of Nesbitt and Leone[8], would predict a rate coefficient of 5.1×10^{-11} cc·molecule^{-1}·sec^{-1}, which is nearly eight times their measured value. A preliminary GEAR simulation predicts that the higher k_2 values suggested by this exercise should produce a faster reagent exhaustion than we observe. At present there is no k_2 value that would appear to satisfy the chain reaction observations in Ref. 8 and in this work and the ratio of R· + Cl_2/O_2 rate coefficients determined by Tyndall et al.[26]

There are no published rate coefficients with which to compare the present k_v measurement; however, it is notable that the value is very near that for HCl(v=1) relaxation by butane.[8] The higher k_v values of Berquist et al.[27] for propane ($k_v = 4.7 \times 10^{-11}$ cc·molecule^{-1}·sec^{-1}) and for isobutene ($k_v = 6.5 \times 10^{-11}$ cc·molecule^{-1}·sec^{-1}) , is almost certainly due to their different experimental method. They produced HCl(v≤7) via a chemical reaction in a fast flow tube reactor and obtained low resolution steady-state emission spectra at varying hydrocarbon concentrations. The spectra were fitted to obtain the relative vibrational populations, and their kinetic rate coefficients were dependent upon these fits and upon a complex kinetic mechanism. The k_v rate coefficient obtained in the present work results from a much more direct measurement. Here only HCl(v≤1) is produced, and the rate coefficient is determined from direct observations of HCl(v=1) fluorescence decays.

The good agreement of k_4 for the cyclohexyl + O_2 addition reaction with two previous measurements[16,24] has been noted. The greatest utility of the laser photolysis/IR

fluorescence technique is that this and other rate coefficients were determined from monitoring the fluorescence emission of a single intermediate, HCl(v=1). With this technique the kinetics of X_2/RH chain reactions (terminated or not) can be studied without the need to monitor other difficult to detect intermediates. Some problems were observed in this study with reagent exhaustion, self-termination, and a thermally driven "hot chain" regime. These effects are discussed below. In theory and in practice this technique would benefit with a more sensitive detector. Effects of each of these problems would be reduced if the experiments could be conducted with better sensitivity at lower chain carrier concentrations.

Though reasonable results were obtained for most of the rate coefficients, the unexpected appearance of the fluorescence profiles needs to be addressed. The profile was predicted to manifest a fast rise at early time followed by a decay to a steady-state level at intermediate time. In contrast, the observed profile exhibited a rise at early time followed by a second rise as if to a steady-state; however, the second rise is cut short by a decay to an apparent steady-state level in the absence of O_2. A factor of two greater k_2 value more closely models the second rise observed in the experimental fluorescence profiles.

The decay following the second rise in the absence of oxygen is much more pronounced than suggested by the simulations (compare Figure 23 to the Figure 20 simulation) so reagent exhaustion alone cannot be the cause. One explanation pursued was self termination of the chain reaction by way of $R\cdot + R\cdot \rightarrow R_2$. This reaction has a rate coefficient as reported by Platz et al.[18] of $(3.0 \pm 0.4) \times 10^{-11}$ cc·molecule^{-1}·sec^{-1}. Another possible reaction that could affect the shape of the fluorescence profile is $RO_2\cdot$ +

RH → ROOH + R·, but this reaction can be ruled out because the rate coefficient[28] (1.58 x 10^{-24} cc·molecule^{-1}·sec^{-1}) is too small for this reaction to greatly modify the chain carrier concentrations. Figure 31 displays the result of three simulations: one under pseudo first-order conditions without the consideration of reagent exhaustion, one with only reagent exhaustion considered, and the other with self termination and reagent exhaustion considered.

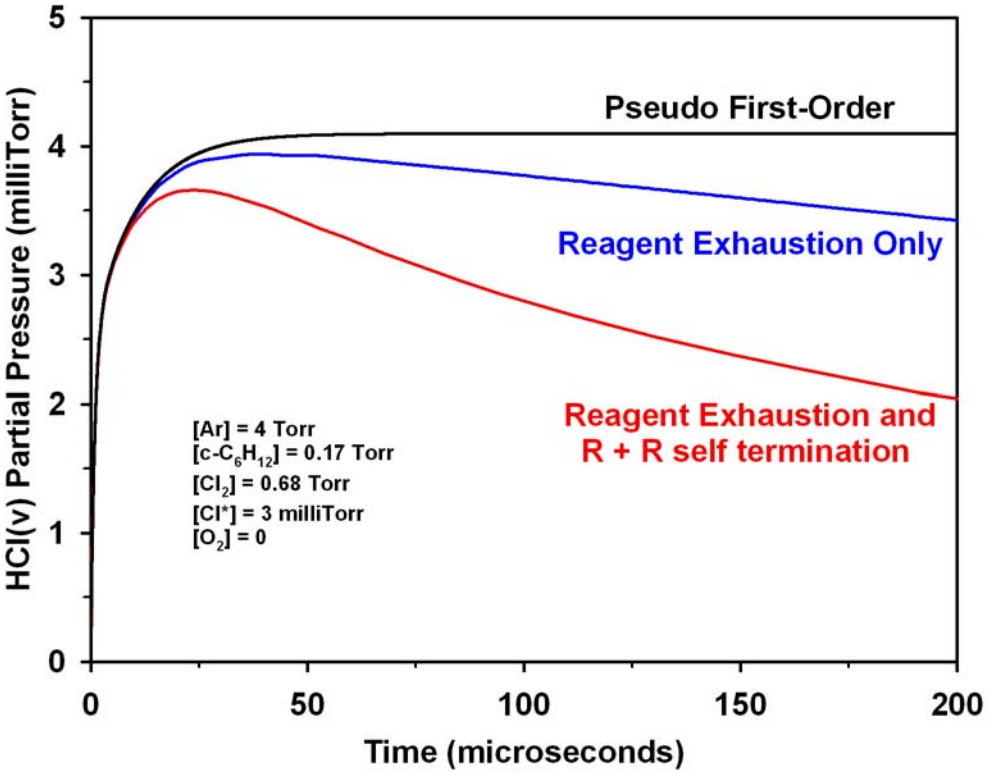

Figure 31: GEAR simulations with reagent exhaustion alone and with the self termination contribution.

It is evident from Figure 31 that self termination via R· + R· → R_2 contributes greatly to the fluorescence profile and is the likely source of the unexpected decay following the second rise in Figure 23. The omission of this reaction from the simulations must be corrected for future work. Of course, this self termination problem would be reduced by

the square of the radical chain carrier concentration if the experiments could be conducted with lower [R·] and higher detection sensitivity.

The difficulty with this study is that reagent concentrations must be maintained as to yield high enough HCl(v) fluorescence intensity as possible for optimal signal-to-noise ratio but without encroaching upon the difficult to model "hot chain" regime. In this regime reagent concentrations are high enough that the combined exothermicity of the propagation steps leads to vibrational and translational heating of products and reactants alike, which thermally drives the kinetics. An example of this regime in the Cl_2/cyclohexane chain reaction is presented in the fluorescence observation of Figure 32 for a gas mixture of approximately 2 Torr Cl_2 and 0.5 Torr cyclohexane in 6.5 Torr Argon. The reactant concentrations are about three times larger here compared to the fluorescence observation in Figure 23, but the Cl_2/cyclohexane ratio is very similar in the two observations. One readily observes that the emission time-scale is tens of milliseconds in Figure 32, which is 100-fold greater than the 400 μs time scale in Figure 23, and that the signal intensity is a factor of 10 greater than in Figure 23. The onset of this "hot chain" emission, it is now believed, provided the apparent steady-state emission level in observations such as that in Figure 23. In the lower argon concentration experiments self-termination caused the signal to decay (unexpectedly) after the second slower rise, but the onset of the "hot chain" behavior prevented the self-termination decay from reaching the zero intensity baseline.

This thermally driven or "hot chain" regime has been described by Nesbitt and Leone[8] in a detailed study of the Cl_2/butane chain reaction. We may make the following parallel conclusions from their work. The limiting hydrocarbon concentration is

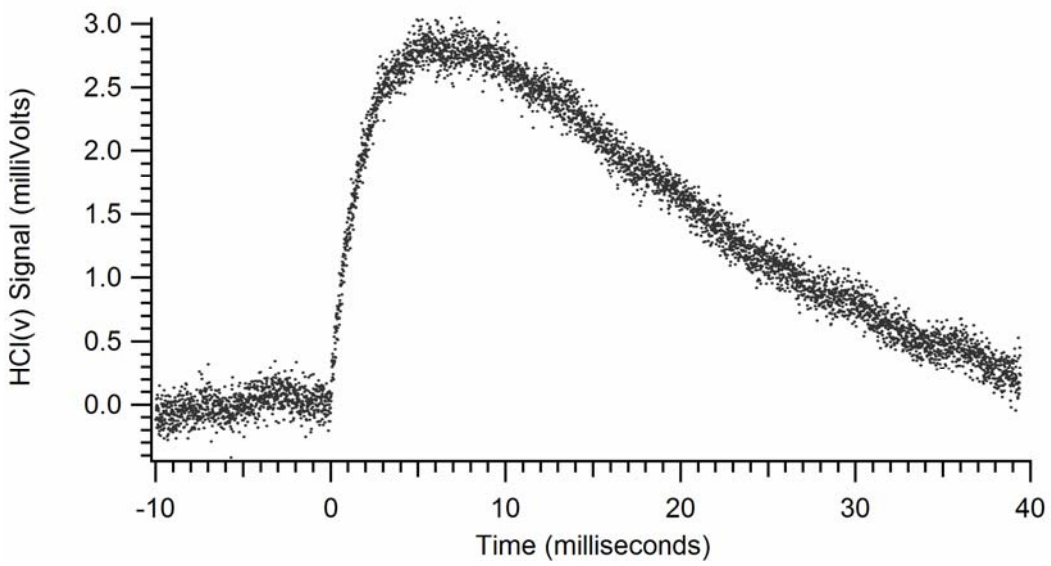

Figure 32: The "hot chain" profile due largely to C-H stretch emission.

consumed early on the time scale of the emission profile, with a time constant of $\tau \approx (k_1 \cdot [Cl\cdot]_0)^{-1}$. This is approximately $\tau \approx 350$ μs for the observation in Figure 35, with 3 milliTorr of Cl· atoms. Thereafter the chain continues with the chlorocyclohexane product as the RH reactant, and then with dichlorocyclohexane isomers, and so on. Most of the emission in Figure 32 is from C-H fluorescence leaking through the narrow-band HCl filter. Nesbitt and Leone[8] continue their article with further insightful consideration of the "hot chain" regime, and the interested reader is invited to continue there. It is sufficient here to invoke this growing IR fluorescence intensity as an artifact that confuses the analysis of the O_2-terminated decays in experiments with lower argon pressures. This underscores the importance of higher argon pressures in experiments designed to determine k_4.

E. Proposed Future Directions

Near the end of this project it became clear that throughout much of this effort the experimental conditions were conducted near the onset of this hot chain regime and may be the reason why the k_2 of $(3.1 \pm 0.2) \times 10^{-11}$ cc·molecule^{-1}·sec^{-1} determined in this study could underestimate the true value. The k_2 experiments should be repeated at higher argon pressures, and both k_2 and k_4 measurements should be replicated before publication.

Additionally, in all future Cl_2/RH chain reaction investigations, smaller concentrations of chlorine atoms must be used in order to minimize the importance of radical self-termination. Smaller chlorine atom concentrations come at a price, which is comparatively smaller signals and lower signal-to-noise ratios. As a consequence, a detector with higher detectivity at 3.5 μm such as indium-antimonide (InSb) would be better suited for this technique for future work.

The terminated Cl_2/cyclohexane chain system was a difficult first system to study because all of the rate coefficients, k_1, k_2, and k_v, had to be determined prior to examining the termination kinetics. A future study of chain termination kinetics would be simplified for a better understood chain system such as Cl_2/n-butane where values for the propagation and relaxation rate coefficients are already available with reasonable certainty.[8]

A brief series of experiments were conducted to examine the termination kinetics in the classic H_2/Cl_2 chain reaction system. HCl(v) fluorescence signals were large and a preliminary evaluation of the O_2-terminated fluorescence decays was consistent with a competitive mechanism, in which both chain carriers (H· and Cl· atoms) combine with oxygen. Neither process dominated under the chain conditions examined in this brief

study. Further investigation of this chain system might be a good undergraduate project. Lastly, for this and for the Cl_2/RH chains termination with other radical scavengers is possible. NO would seem to be first in line for future chain termination efforts. Several $R\cdot + \cdot NO \rightarrow RNO$ rate coefficients might be determined for use in atmospheric modeling codes.

REFERENCES

1. *Oxford Dictionary of Chemistry*. Oxford University Press, 2004.

2. Andrews, D.L. *Lasers in Chemistry, 3rd Ed* . ; Springer, New York, 1997.

3. Seinfeld, J.H.; Pandis, S.N. *Atmospheric Chemistry and Physics: From Air Pollution to Climate Change*.; John Wiley & Sons, Inc., New York, 1998.

4. Semenov, N. N. *Chemical Kinetics and Chain Reactions*, Clarendon, Oxford, 1935.

5. Setser, D. W., ed. *Reactive intermediates in the gas phase: generation and monitoring*, Academic Press, New York, 1979.

6. Nesbitt, D. J.; Leone, S. R. *J. Chem. Phys.* **1980**, *72*, 1722-1732.

7. Nesbitt, D. J.; Leone, S. R. *J. Chem. Phys.* **1981**, *75*, 4949-4959.

8. Nesbitt, D. J.; Leone, S. R. *J. Phys. Chem.* **1982**, *86*, 4962-4973.

9. Dolson, D. A.; Leone, S. R. *J. Chem. Phys.* **1982**, *77*, 4009-4021.

10. Dolson, D. A.; Leone, S. R. *J. Phys. Chem.* **1987**, *91*, 3543-3550.

11. (a) Klingshirn, Michelle D. *Laser Initiated Chemical Chain Reactions: Termination Kinetics of the Cl_2/HBr/NO Chain System* . M.S. Thesis, Wright State University, 1992. (b) Dolson, D.A. , Klingshirn, M.D. *J. Phys. Chem.* **1993**, *97*, 6645-6649.

12. NIST Chemistry WebBook, http://webbook.nist.gov/chemistry/, accessed April, 2007.

13. B. Egger, K. W.; Cocks, A. T. *Helv. Chim. Acta* **1973**, *56*, 1516-1536, as quoted by Gordon, A. S.; Smith A. Reuven J. Phys. Chem. **1962**, *66*, 521-524.

14. Braithwaite, M. ; Leone, S. *J. Chem. Phys.* **1978**, *69*, 839-845 .

15. Sander, S. P., B. J. Finlayson-Pitts, R. R. Friedl, D. M. Golden, R. E. Huie, C. E.

Kolb, M. J. Kurylo, M. J., Molina, G. K. Moortgat, V. L. Orkin and A. R. Ravishankara *Chemical Kinetics and Photochemical Data for Use in Atmospheric Studies, Evaluation Number 14*. JPL Publication 02-25, Jet Propulsion Laboratory, Pasadena, 2002.

16. Platz, J.; Sehested, J.; Nielsen, O.J.; Wallington, T.J. *J. Phys. Chem. A* **1999**, *103*, 2688-2695 .
17. GEAR ITERATOR, program number QCMP022 from the Quantum Chemistry Program Exchange at Indiana University, Bloomington, IN. URL: http://qcpe.chem.indiana.edu/ (accessed April, 2007).
18. Leone, S. R. *J. Phys. Chem. Ref. Data* **1982**, 11, 953-996.
19. Atkinson, R.; Baulch, D.L.; Cox, R.A.; Hampson, R.F., Jr.; Kerr, J.A.; Rossi, M.J.; Troe, J. *Phys. Chem. Ref. Data* **1997**, *26*, 521-1011.
20. Hussong, Karen. *Experimental Determination of the Cl Atom Quantum Yield From S_2Cl_2 and SCl_2 at 355 and 266 nm*. M.S. Thesis, Wright State University, 1994.
21. Seery, D.; Britton, D. *J. Phys. Chem.* **1964**, *68*, 2263-2266 .
22. Okabe, H. *Photochemistry of Small Molecules*. ; John Wiley & Sons, Inc., New York, 1978.
23. Davis, D. D.; Braun, W.; Bass, A. M. *Int. J. Chem. Kinet.* **1970**, *2*.
24. Wu, D.; Bayes, K. D. *Int. J. Chem. Kinet.* **1986**, *18*, 547-554.
25. NIST Chemical Kinetics Database, http://kinetics.nist.gov/kinetics/index.jsp, accessed May, 2007.
26. Tyndall, G.S.; Orlando, J.J.; Wallington, T. J.; Dill, M. Kaiser, E. W. *Int. J. Chem. Kinet.* **1997**, *29*, 43-55.

27. Berquist, B. M.; Bozzelli, J. W.; Dzelzkalns, L. S.; Piper, L. G.; Kaufman, F. *J. Chem. Phys.* **1982**, *76*, 2984-2992.

28. Hermans, et al. *Chem. Phys. Phys. Chem.* **2005**, *6*, 637-645.

A1. Riemschneider, R. Ann. **1952**, *576*, 94-103.

A2. Riemschneider, R. *Monatshefte fuer Chemie* **1955**, *86*, 101-116.

Appendix: Heterogeneous Photochemistry on the Cell Windows

Undesired heterogeneous photochemical reactions proved to be a problem on the inner surface of the fused silica windows through which the UV laser beam entered and exited the cell. After an extended set of experiments with 355 nm photolysis of 0.74 Torr chlorine, 0.16 Torr cyclohexane, 3.8 Torr argon and up to 0.2 Torr oxygen, small specks of a white solid substance was noted on the windows in addition to an oily liquid. The white solid is noticeable in the photograph of the demounted window presented in Figure A1.

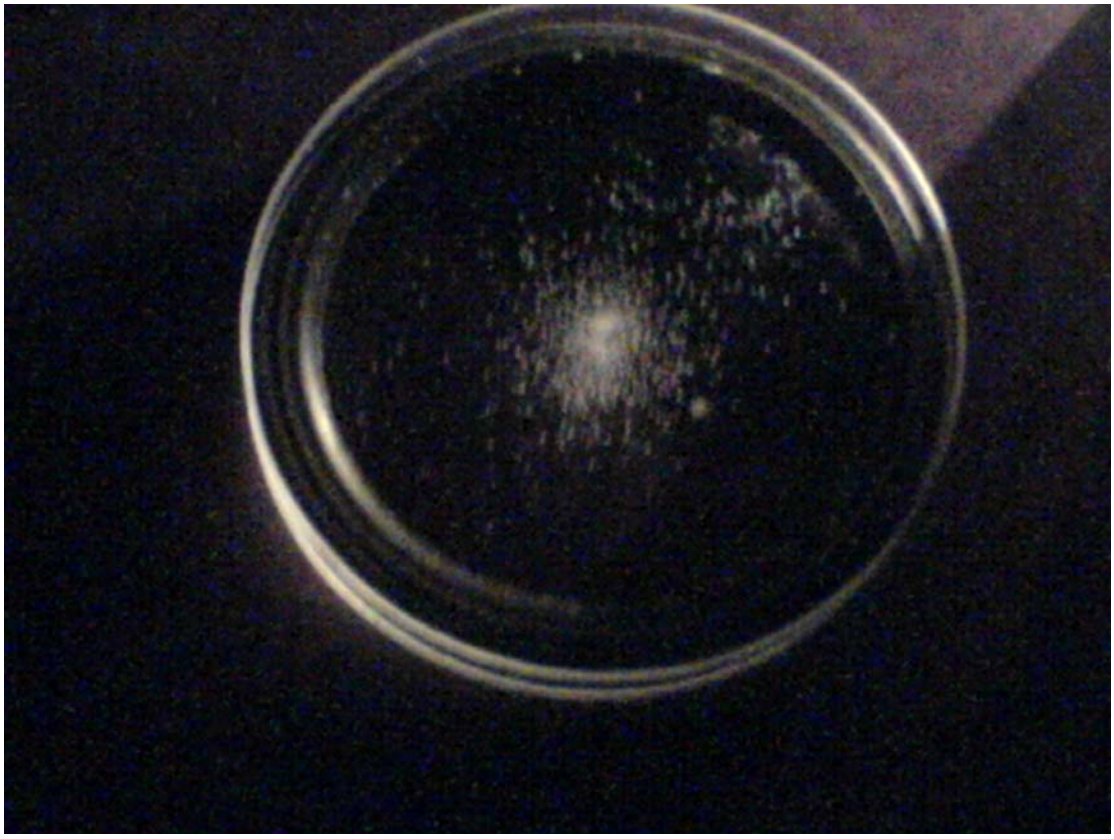

Fig. A1. Photograph of 38 mm diameter fused silica window resting on an o-ring. The white photochemical product is apparent.

The white substance was dissolved in dichloromethane and subjected to GC/MS analysis. Unavoidably, some of the oily liquid was probably included in this sample. The chromatogram (total ion current vs. retention time, t_R) is presented in Figure A2.

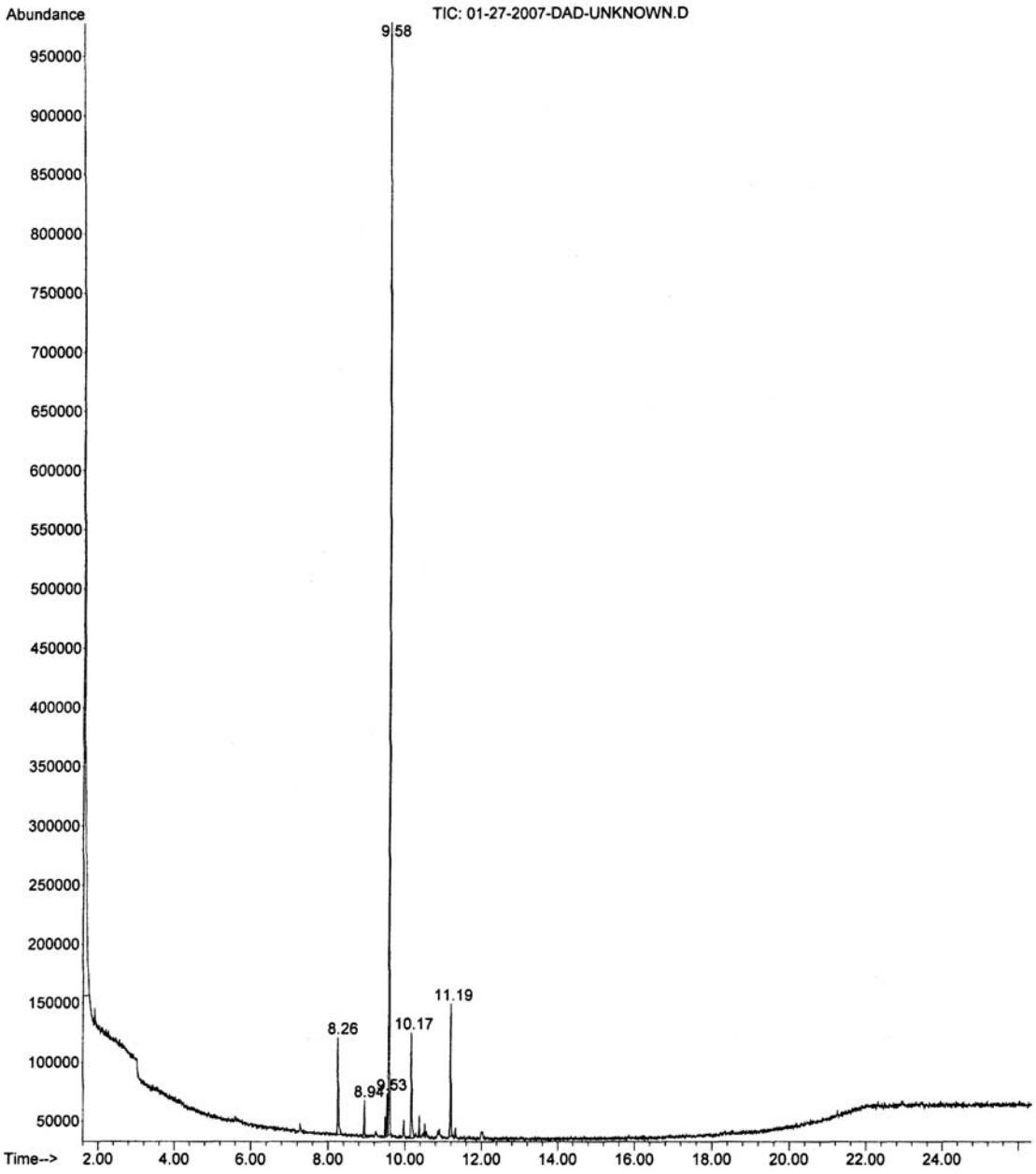

Figure A2. Gas chromatogram of photochemical deposits on the reaction cell windows.

Approximately 95% of the total peak area in the t_R = 8-12 minute range is contained in only four peaks: Compound 1 (t_R = 8.28 min, 7.4% area), Compound 2 (t_R = 9.58 min, 69.6% area), Compound 3 (t_R = 10.16 min, 8.3% area) and Compound 4 (t_R = 11.19 min, 9.4% area). The mass spectrum of the most prevalent Compound 2 is presented in Figure A3, and the m/z peaks are identified in Table A1.

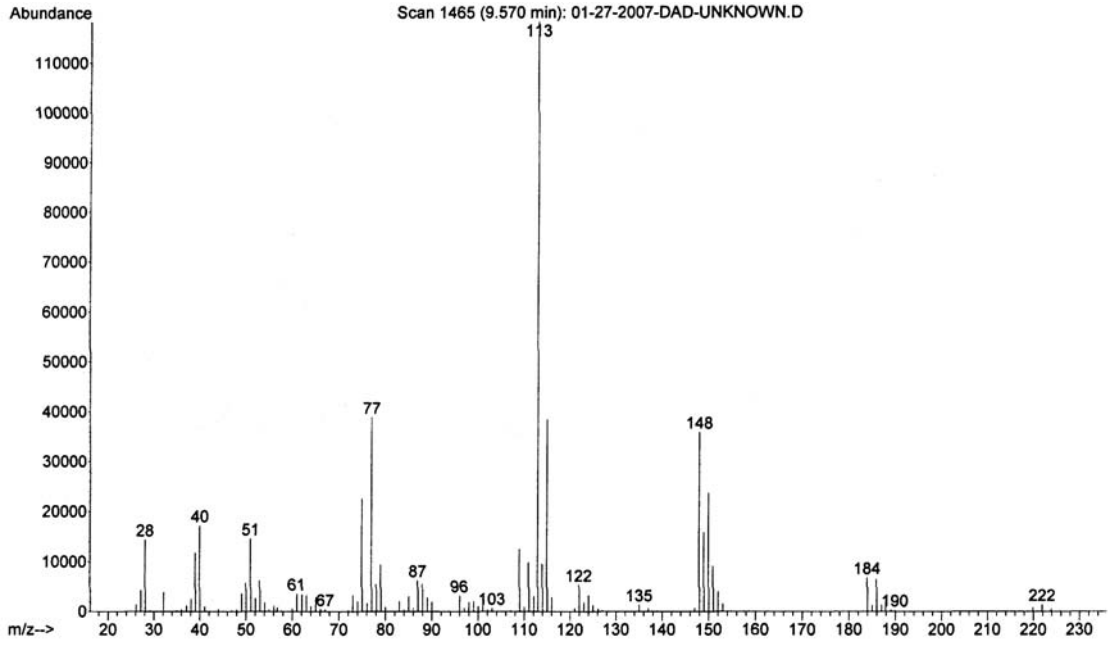

Figure A3. Mass spectrum of Compound 2.

Table A1. m/z Peaks in the Mass Spectrum of Compound 2

m/z [a]	probable identity	Cl isotopomer ratios
220	M = $C_6H_8{}^{35}Cl_4$	220:222:224 ≈ consistent with 3:4:2 (calc)
184	M – 36 (HCl)	184:186:188 ≈ 4:4:1 (obs) ≈ 3.3:3.2:1 (calc)
148	184 – 36 (HCl)	148:150:152 = 9.3:6.1:1 (obs) ≈ 9.5:6.2:1 (calc)
113	148 – 35 (Cl)	113:115 = 3.1:1 (obs) = 3.1:1 (calc)
77	113 – 36 (HCl)	

a m/z values based upon ^{35}Cl isotope

The highest mass values are found in a set of three small intensity peaks at m/z = 220, 222 and 224. The m/z = 220 peak is consistent with the formula, $C_6H_8{}^{35}Cl_4$, and the m/z = 220:222:224 intensity profile of the three peaks is consistent with the 3:4:2 ratio expected for the $^{35}Cl_4$: $^{35}Cl_3{}^{37}Cl$: $^{35}Cl_2{}^{37}Cl_2$ substitution. Higher numbers of the ^{37}Cl isotope in this compound have very low abundances and the m/z = 226 and 228 peaks are not observed. Other major m/z peaks in the mass spectrum of Compound 2 are consistent with losses of Cl or HCl. The m/z = 77 fragment ion ($C_6H_5{}^+$) exhibits no chlorine isotope pattern.

The interpretation of the mass spectrum of Compound 2 supports the conclusion that the major photochemical product on the windows is tetrachlorocyclohexane, but nothing more was determined regarding specific isomers. Further support for this conclusion is found in literature accounts of chlorination experiments with liquid cyclohexane, in which tetrachlorocyclohexane was found to be a major cyclohexane chlorination product. [A1,A2] The mass spectrum for Compounds 1, 3 and 4 are consistent with dichloro, trichloro and tetrachloro substituted cyclohexenes: $C_6H_8Cl_2$, $C_6H_7Cl_3$, and $C_6H_6Cl_4$.

Given the nature of the gas mixture and the UV photolysis wavelength these findings are not a surprise. Undoubtedly the reactions at the windows have a heterogeneous mechanism wherein cyclohexane and its chlorinated products (and perhaps chlorine as well) have some affinity for the window surface, which allows for the multiple chlorination events. This laser photochemical route to the chlorinated cyclohexane and cyclohexenes is perhaps the most expensive synthesis of such products. While this problem appears to be isolated at the windows, the presence of these

hydrocarbon compounds in the cell is undesired and the solid deposits attenuate and scatter the laser beam so that IR fluorescence signals are reduced. For these reasons a redesign of the reaction cell, to allow for an argon stream to be directed onto the windows, might minimize this problem in future work.